A

DISSERTATION REPORT

ON

# ISOLATION ENHANCEMENT IN MIMO ANTENNA SYSTEM FOR 5G WIRELESS APPLICATIONS

*is submitted in partial fulfillment for the award of degree of*

**MASTER OF TECHNOLOGY**

IN

**ELECTRONICS AND COMMUNICATION**

BY

**DURGA KUMARI**

(2015PEC5307)

UNDER THE GUIDANCE OF

**Prof. K. K. SHARMA**

(H.O.D., ECE, M.N.I.T. JAIPUR)


DEPARTMENT OF ELECTRONICS AND COMMUNICATION ENGINEERING

MALAVIYA NATIONAL INSTITUTE OF TECHNOLOGY JAIPUR

JUNE 2017

**DEPARTMENT OF ELECTRONICS AND COMMUNICATION ENGINEERING**

**MALAVIYA NATIONAL INSTITUTE OF TECHNOLOGY**

**JAIPUR (RAJASTHAN)-302017**

## ***CERTIFICATE***

This is to certify that the dissertation report entitled "**Isolation Enhacement in MIMO Antenna System for 5G wireless applications"** submitted by **DURGA KUMARI** (2015PEC5307), in partial fulfillment of Degree **Master of Technology** in **Electronics & Communication Engineering** during the academic year **2016-2017**. To best of my knowledge and belief that this work has not been submitted elsewhere for the award of any other degree. The work carried out by her has been found satisfactory under my guidance and supervision in the department and is approved for submission.

Date:

Place: MNIT Jaipur

**Prof. K. K. SHARMA**
Professor
Department of ECE
M.N.I.T. JAIPUR

**DEPARTMENT OF ELECTRONICS AND COMMUNICATION ENGINEERING**

**MALAVIYA NATIONAL INSTITUTE OF TECHNOLOGY**

**JAIPUR (RAJASTHAN)-302017**

## ***CANDIDATE DECLARATION***

This is to certify that the dissertation report entitled "**Isolation Enhacement in MIMO Antenna System for 5G wireless applications**" being submitted by me in partial fulfillment of degree of **Master of Technology** in **Electronics & Communications** during **2016-2017** in a research work carried out by me under supervision of **Prof. K. K. SHARMA** and content of this dissertation work in full or in parts have not been submitted to any other institute or university for award of any degree or diploma. I also certify that no part of this dissertation work has been copied or borrowed from anywhere else. In case any type of plagiarism is found out. I will be solely and completely responsible for it.

Date: **DURGA KUMARI**

Place: M.Tech (ECE)

2015PEC5307

MNIT Jaipur

# ACKNOWLEDGEMENT

I would like to convey my thanks and appreciation to my supervisor, **Prof. K. K. SHARMA** for giving me the favorable time to work under his direction. He had encouraged me in the period of disquietude and mentors me to carry on this research work. He had provided a lot of information and advice on the project, without that I could not have completed project work.

I must recognize the support and guidance of all staff members of Department of Electronics & Communication. I am sincerely thankful to research scholars **Mr. Muquaddar Ali** & **Mr. Varun Setia** for their constant support and I am also very much thankful to my friends who helped me to understand basic concepts and always encouraged me during work. I am very much appreciative of my friends for their generosity, guidance, and proficiency.

And at last but not the least my parents and my husband who supported me in all way and always encouraged me at each and every step of my career I express my great respect for them.

DURGA KUMARI

2015PEC5307

# CONTENTS

# LIST OF FIGURES

# LIST OF TABLES

# LIST OF ABBREVIATIONS

| | |
|---|---|
| MIMO | Multiple output multiple input |
| MoM | Method of moments |
| TARC | Total active reflection coefficient |
| DG | Directive gain |
| ME | Multiplexing efficiency |
| MEG | Mean effective gain |
| CST | Computer simulation technology |
| SMLR | Slotted Meander Line Resonator |

# ABSTRACT

Availability of unlicensed 60 GHz frequency band has attracted considerable attention for various indoor applications such as WLAN, WPAN, and wireless uncompressed HDTV. This frequency band provides a high data rate communication with a large number of users. Despite its unique potential to support high data rate communications, there are some limitations for developing 60 GHz mm-wave communication system due to the high amount of propagation loss. To overcome this drawback, MIMO (Multiple Input Multiple Output) technology offers the promising approach to enhance link performance.

MIMO technology uses multiple antennas at transmitter and receiver side to enhance the channel capacity for delivering high data rate without the need of additional power or frequency band. When multiple antennas are closely fitted within a standard enclosure, mutual coupling between antennas degrade the performance of antenna system. To avoid mutual coupling between the antenna array slotted meander line resonator and metamaterial are frequently used.

The aim of this thesis work is to design the MIMO antenna array with improved isolation at 60 GHz for 5G wireless communication. For this purpose an antenna of I-shaped patch is designed at 60 GHz on RT Duroid having permittivity 2.2. For optimization of design, the slot is cut in the upper arm of I-shaped patch antenna of length $\lambda$, $\lambda/2$, $\lambda/4$, $\lambda/8$. The comparative study among slots and without slot shows that the slot length $\lambda/4$ is giving best return loss of – 41 dB lower than the remaining slots. The optimized antenna is utilized for MIMO antenna array by constructing multiple antennas on same extended substrate RT Duroid and Ground. The impact of mutual coupling is analyzed for spacing greater and less than $\lambda/2$ . By analyzing the results, placing antenna array elements less than $\lambda/2$ degrades the performance of MIMO antenna system due to mutual coupling. To improve the isolation between the MIMO antenna array, the techniques of slotted meander line resonator and metamaterial are investigated for $1\times 2$ array. A comparative study between these two isolation techniques demonstrate that the metamaterial is providing 10 dB more isolation than the slotted meander line resonator at the cost of decreasing the matching bandwidth. The antenna array of $1\times4$ is then investigated for

MIMO application using SMLR. We are able to achieve isolation of the order of -25 dB which is higher than the reported value in the existing literature. The total area covered by the $1 \times 4$ MIMO antenn array is $28.37 \times 8.314$ $mm^2$.

# CHAPTER 1

# INTRODUCTION

## 1.1 Introduction

Antenna plays a vital role in the wireless communication systems. The performance of antenna significantly enhances the characteristics of wireless communication. For some applications, the single antenna does not meet the requirement of antenna gain and radiation pattern. Hence there is a need for multiple antennas to meet this requirement. Hence MIMO is the technique to improve system performance [1]. Multiple input and multiple output (MIMO) consists of multiple antennas at both receiver and transmitter to enhance the channel capacity without the need of additional power or frequency band.

To increase the signal-to-noise ratio and channel capacity, the distance between the antenna elements should be greater than $\lambda/2$. Due to space limitation, the antennas are closely packed inside a wireless device. Closely packing of antenna array leads to a mutual coupling which degrades the radiation pattern, antenna gain, operational bandwidth and radiation efficiency.

Mutual coupling refers to the phenomena of the interaction of electromagnetic waves between antenna elements. This is undesirable because the energy that should be radiated away is absorbed by near by antenna. It affects the antenna array performance in the following ways: changes the antenna radiation pattern, changes the input impedance. The mutual coupling depends on orientation and spacing between antenna elements.

A lot of work has been done to eradicate the problem of mutual coupling such as Mushroom like EBG structure, defected ground plane with notch filter property, neutralization line. The mentioned solution works for low operating frequency. So, for isolation enhancement at high operating frequency different techniques are utilized such as Slotted meander line structure [2], [3] and metamaterial [4], [5].

The unlicensed 60 GHz band has attracted a lot of attention because of the large bandwidth (57-64 GHz), high data rate 40-50 times faster than current WLAN

technologies which result into high definition video streaming, wireless gaming, mobile distributed computing, fast large file transfer in milliseconds, internet access. Millimeter wave has high attenuation by walls, rain, fog, snow, atmospheric gases result into frequency reuse over small distances [6-8]. For the MIMO antenna system for 5G wireless communication at 60 GHz, it is mandatory to reduce the coupling between the antenna elements[9-11].

Firstly, to reduce the mutual coupling between antenna elements Slotted meander line resonators (SMLR) is designed between the antenna elements. These SMLR act as a bandstop resonator that specifically stops the surface current from one unit cell to another unit cell.

Secondly, Metamaterials can be used in different applications such as beamforming and miniaturization. Here it is utilized as a bandstop resonator to improve isolation for miniaturization.

## 1.2 Objective of Thesis

The objective of this thesis work is to study the impact of mutual coupling among antenna arrays. Firstly, the designing of the antenna at single 60 GHz band with optimized dimensions is taken into consideration. Secondly, the designing of an antenna array with and without isolation technique with the comparative study is done. Finally, the effect of different isolation techniques in MIMO antennas is compared, and the conclusion is drawn. The simulations results are carried out in CST Studio.

# CHAPTER-2

# BASIC THEORY

The unprecedented growth in the wireless communication technologies internationally has opened an immense commercial opportunity for the mobile industry. Over recent years, due to the rapid evolution of wireless service applications made industries to develop miniaturized and portable devices [1]. Hence, it is important for us to provide antenna configuration with compact size and light weight.

The antenna is a device which converts electrical energy into electromagnetic waves and vice-versa. Due to compact and low profile, microstrip patch antenna is very popular nowadays.

## 2.1 Microstrip patch antenna

In this chapter, Microstrip Patch Antenna is followed by advantages, disadvantages, and applications. Next, some feed modeling techniques are discussed. Finally, a detailed explanation of Microstrip patch antenna analysis, its theory, and the working mechanism is explained [12].

### 2.1.1. Overview

Microstrip patch antenna consists of a patch on one side of a dielectric substrate which has ground plane on another side as shown in fig. 2.1**.** The patch acts as a radiator. It is made up of conducting material like gold, copper, silver, etc. and can take any possible shape. The feed lines and patch are usually photo-etched on the dielectric substrate.

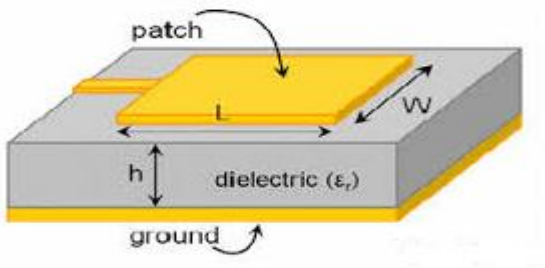


Fig. 2.1 Proposed microstrip patch antenna

In order to simplify the analysis, the patch shape is generally circular, triangular, rectangular, elliptical, square or some other shape as shown in fig.2.2. For a rectangular patch, the patch is very thin $t << \lambda$ (where t is the thickness of patch) and the length is $(\lambda /3) < L < (\lambda/2)$. The height of substrate selected is $0.003\ \lambda \leq h \leq 0.05\ \lambda$ and the dielectric constant lies between 2.2 to 12.

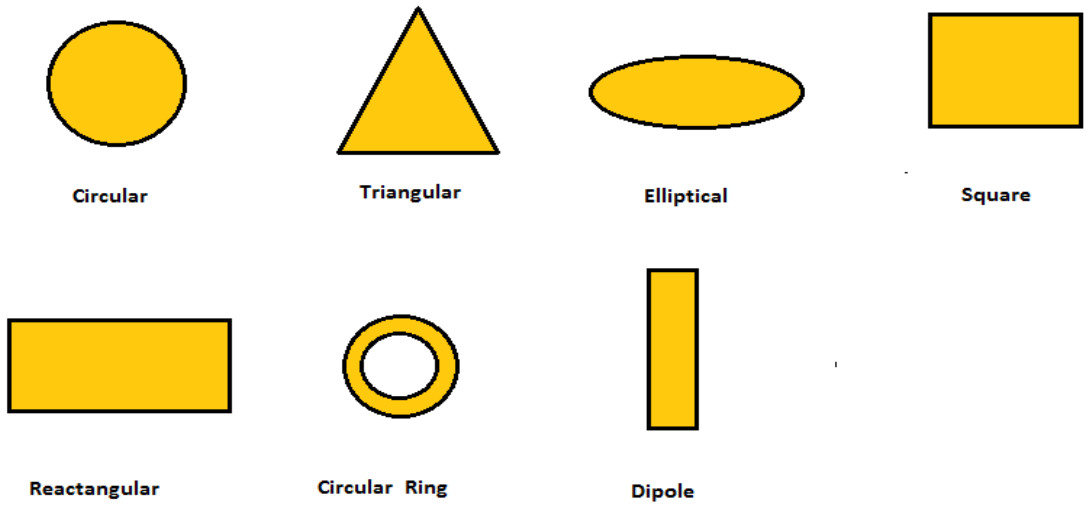


Fig 2.2 Common shapes of microstrip patch antennas

The radiation characteristic of microstrip patch antenna is because of the fringing fields exist between the ground plane and patch edge. For good antenna performance, a thick substrate is desired to have low dielectric constant. Since the height of substrate is directly proportional to efficiency, better radiation, larger bandwidth. The thick dielectric substrate configuration leads to larger antenna size. To minimize the size, higher dielectric constant with thin substrate must be used which leads to narrower operational bandwidth and less efficient. Hence a compromise is there in antenna performance and antenna size.

### 2.1.2 Advantages

- lighter in weight, low cost, low volume, low profile, smaller in dimension and are easy to fabricate
- Compatible with microwave and millimeter-wave integrated circuits (MMIC) and have the ability to conform to planar and non-planar surfaces.
- There is no requirement of cavity backing

- When particular mode and shape is selected, different resonant frequency, polarization pattern, and impedance are obtained.
- When mounted on rigid surfaces it is mechanically robust.
- High performance
- Easily integrated with microwave integrated circuits (MICs).

### 2.1.3 Disadvantages

- Low power
- Low efficiency
- Poor polarization purity
- Poor scan performance
- Spurious feed radiation
- Narrow frequency bandwidth
- High-Quality factor (sometimes excess of 100)

### 2.1.4 Applications

- Used in mobile satellite communication system
- Direct broadcast television system
- Used in WLANs, WiMAX,
- Feed elements in coaxial system
- Wifi and GPS system.
- Missiles and telemetry
- A non-medical based application such as medical hyperthermia.

### 2.1.5 Feeding Techniques

Microstrip patch antennas can be fed by a variety of methods i.e.

1] Contacting.

- Coaxial probe feed
- Microstrip feed

2] Non-Contacting.

- Aperture coupling
- Proximity coupling feed

**a) Microstrip Line Feed**

In this method, a conducting strip is connected directly to the edge of the patch as shown in fig.2.3. The width of conducting strip is smaller as compared to the radiating patch, and such type of structure has the advantage that the patch and feed can be etched on the same substrate to provide a planar structure. For impedance matching inset cut in the patch is made to avoid additional matching elements. This is achieved by properly controlling inset position and size. However, increase in the substrate thickness give rise to the spurious feed radiation and surface waves and reduces operating bandwidth which is undesired. This feeding technique gives ease of fabrication and provides better impedance matching than other techniques. The feed radiation leads to undesired cross polarization.

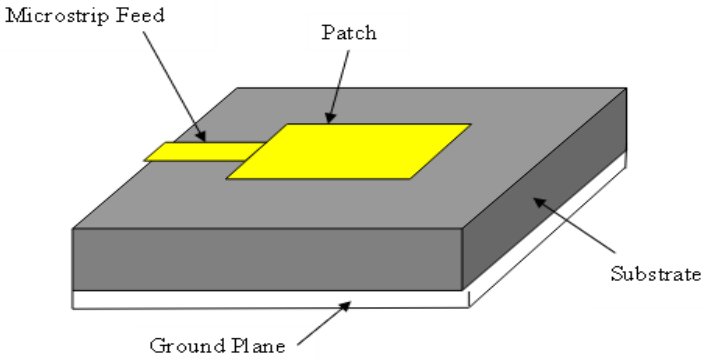


Fig. 2.3 Microstrip line feed

**b) Coaxial feed**

It is a very common technique for feeding the microstrip patch antenna. As seen from fig.2.4 the inner conductor of coaxial cable extends through the dielectric substrate, and it is soldered to radiating patch. The outer conductor soldered to the ground.

The advantage of this feeding technique is that the feed can be placed at any desired location inside the patch to match input impedance. But main disadvantage of this technique is that it provides narrow bandwidth and difficult to drill a hole in the thick substrate and not having a planar structure.

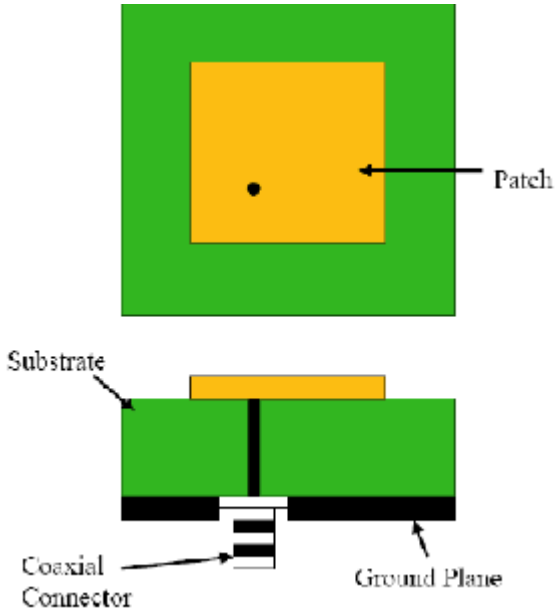


Fig. 2.4 Probe fed microstrip patch antenna

**c) Aperture-Coupled feed**

This feeding technique consists of the radiating patch and microstrip feed line are separated by ground plane as shown in fig. 2.5 Coupling between patch and microstrip feed line is made through a slot or aperture in the ground plane. The slot is usually centered under the patch, leads to lower cross-polarization due to the symmetry of configuration. The amount of coupling is determined by size, shape, and location of the aperture. Spurious radiation is minimized in this case since feed line and patch separated by ground. The patch is placed over a high dielectric substrate which is separated by lower dielectric substrate through the ground plane. This feeding technique suffers from the disadvantage of multiple layers of a dielectric substrate which is difficult to fabricate. Hence, the overall weight of antenna increases. It also provides narrow bandwidth.

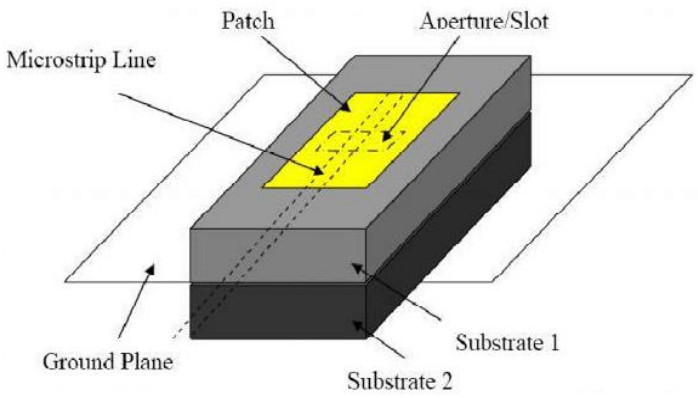


Fig. 2.5 Aperture coupled feed

### d) Proximity Coupled Feed

This feeding technique also called as electromagnetic coupling scheme. The proximity coupled feed shown in fig. 2.6. Unlike the Aperture coupling, it does not have ground plane to separate the two dielectric substrates. The main advantage is that it eliminates the spurious feed radiation and offers very large bandwidth. Impedance matching can be achieved by controlling the width to the line ratio of the radiating patch and the length of feed line. The disadvantage of this feeding technique is the fabrication of two substrates with proper alignment. Because of the two substrates the overall weight and size increases.

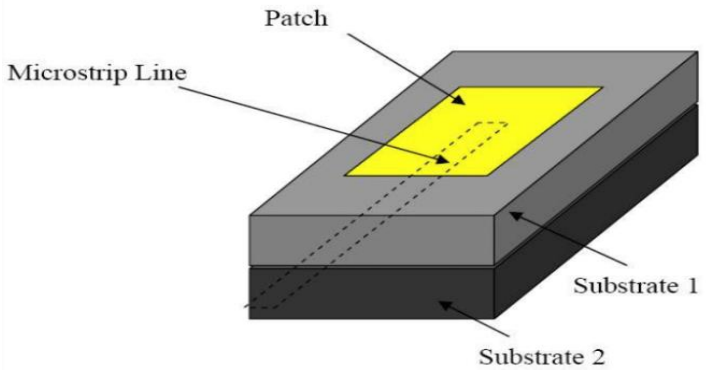


Fig 2.6 Proximity coupled feed

### 2.1.6 Method of analysis

The model for the analysis of Microstrip patch antennas is the transmission line model, cavity model, and full wave model. Transmission line model is less accurate but gives good physical insight and simplest of all. The cavity model is more accurate than transmission line model and gives good physical insight but complex in nature. The full wave model is extremely accurate, versatile and can treat any configuration of the antenna but it gives less insight as compared to the two models mentioned above and is far more complex in nature.

#### a) Transmission line model

It represents two slots of microstrip patch antenna, height h, and width W, separated by a transmission line of length L as shown in fig. 2.7

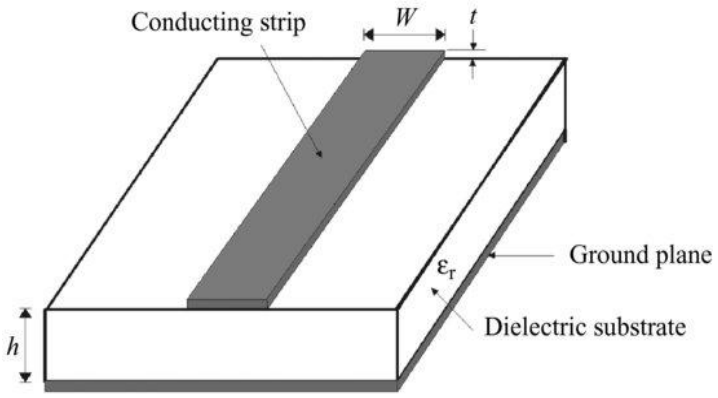


Fig. 2.7 Microstrip line

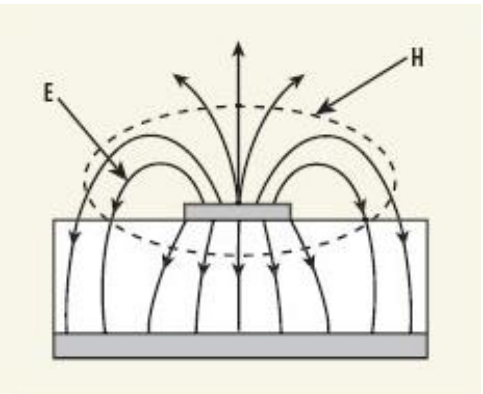


Fig. 2.8 Electric field lines in microstrip feed

From fig.2.8 it is concluded that the most of the electric field lines confined to the substrate and parts of some line in the air. The phase velocity is different in substrate and air so, the transmission line cannot support pure transverse electric magnetic (TEM) mode of propagation. Instead of this, the dominant mode of propagation would be quasi-TEM mode. Hence, there must be an effective dielectric constant ($\varepsilon_{reff}$) obtained for fringing and the wave propagation in line. The value of $\varepsilon_{reff}$ is always less than $\varepsilon_r$ because fringing field of the patch is not confined in the dielectric but also spreads out in air as shown in fig. 2.8 the expression for $\varepsilon_{reff}$ is given by **C.A. Balanis**

$$\varepsilon_{reff} = \frac{\varepsilon_r+1}{2} + \frac{\varepsilon_r-1}{2}\left[1 + 12\frac{h}{W}\right]^{-\frac{1}{2}}$$

Where, $\varepsilon_{reff}$ = Effective dielectric constant

$\varepsilon_r$ = Dielectric constant of substrate

h = Height of dielectric substrate

W = Width of patch

The wavelength in the dielectric substrate,

$$\lambda = \frac{\lambda_0}{\sqrt{\varepsilon_{reff}}}\,;\, \frac{W}{h} > 1$$

$\lambda_0$ = free space wavelength

To operate in the fundamental $TM_{10}$ mode, the length of the patch must be

$0.33\lambda_0 < L < 0.5\lambda_0$

The microstrip patch antenna as shown in fig.2.9 has two slots, separated by a transmission line of length L and open circuited at both the ends. With respect to the ground plane, the field at the edges can be resolved into normal and tangential components.

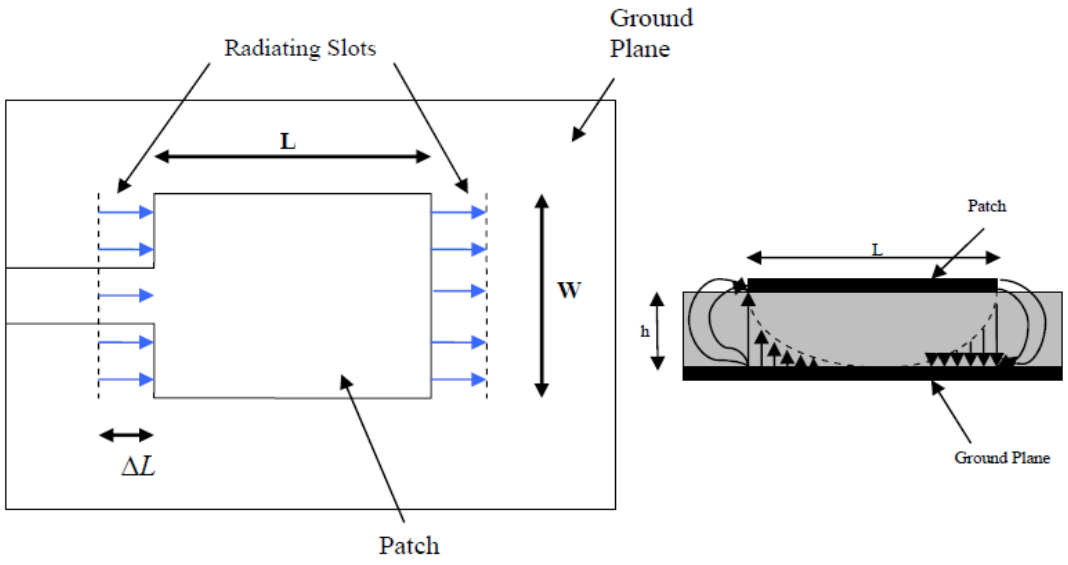


Fig. 2.9 Top view and side view of antenna

In the broadside direction, the normal components of electric field cancel each other at the two edges which are in opposite directions and out of phase since the length of the patch is λ/2. The tangential components are in phase which additively gives maximum radiation pattern to the normal of the patch surface. Electrically the length of patch antenna looks slightly greater than physical length. The extended length at both the ends of length L is given by Hammerstad as:

$$\Delta L = 0.412\ h\ \frac{(\varepsilon_{reff}+0.3)(\frac{W}{h}+0.264)}{(\varepsilon_{reff}-.258)(\frac{W}{h}+0.8)}$$

The effective length $L_{eff} = L + 2\Delta L$

Effective length for a given resonant frequency $L_{eff} = \frac{c}{2f_0\sqrt{\varepsilon_{reff}}}$

For rectangular microstrip patch antenna the $T_{mn}$ mode resonance frequency

$$f_0 = \frac{c}{2\sqrt{\varepsilon_{reff}}}\left[\left(\frac{m}{L}\right)+\left(\frac{n}{W}\right)\right]^{\frac{1}{2}}$$

For efficient radiation, $W = \frac{c}{2f_0\sqrt{\frac{(\varepsilon_r+1)}{2}}}$

### b) Cavity model

Transmission line avoids field variation along the radiating edges. This disadvantage can be overcome by using cavity model. In this model, the microstrip patch antennas resemble as dielectric-loaded cavities. The inner region of the dielectric substrate is modeled as cavity bounded with the top region and bottom region by electric walls and along the periphery of the patch by the magnetic wall. The basic assumption for this model is the height of the substrate is h << λ. Because of this, the field variation is almost null to the normal of the patch. In this, the field is almost concentrated in the cavity and radiation take place from side walls as shown in fig. 2.10 This model involves two mechanisms attractive and repulsive. An attractive mechanism exists in the opposite charges between patch and ground. A repulsive mechanism exists in the like charges between upper and lower of patch charges. This model assumes that the height to width ratio is very small and it results into dominance of attractive mechanism which leads to most of the current and the charge concentration beneath the patch. This model is suitable for circular, ellipse, discs, square, etc.

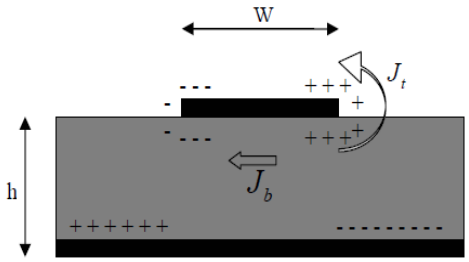


Fig. 2.10 Charge distribution and current density in microstrip patch antenna

### c) Full Wave Solutions – Method of Moments

In MoM, the volume polarization currents are used to model the fields in the dielectric substrate and surface currents are used to model microstrip patch. Newman and Tulyathan have shown that how an integral equation is obtained for these unknown currents and by using the MoM, these electric field equations are converted into matrix form which can then be solved by any mathematical method and yields the result.

## 2.2 Antenna parameters

For designing of an antenna, there is certain parameters requirement which describes the configuration of the antenna.

### 2.2.1 Radiation Pattern

The radiation pattern is defined as the "a graphical and mathematical function of the radiation properties of the antenna as a function of space coordinates. In most of the cases, the radiation pattern is determined in the far-field region and is represented as a function of the directional coordinate. Radiation properties include power flux density, field strength, phase or polarization, directivity, radiation intensity."

The radiation pattern is a 3-D pictorial representation of the power transmitted or received as a function of angular position and radial distance from the antenna. Radiation pattern consists of the main lobe, side lobes, and back lobes. The side lobes and the back lobes are the undesirable lobes which deteriorate the performance of an antenna by wasting the transmitter power and becomes the source of the noise.

### 2.2.2 Return Loss

It shows the loss of power that is reflected back due to discontinuity in the transmission line. The occurrence of discontinuity is because of mismatch of the load. It is expressed in dB,

$$R_L = -20\log_{10}|\Gamma|(dB)$$

Where, $|\Gamma| = \frac{V_0^-}{V_0^+} = \frac{Z_L - Z_0}{Z_L + Z_0}$

$|\Gamma|$ = Reflection coefficient

$V_0^-$ = Reflected voltage

$V_0^+$ = Incident voltage

$Z_L$ = Load impedance

$Z_0$ = Characteristic impedance

Return loss is a measure of how well the device is matched.

### 2.2.3 Gain and Directivity

The directive gain of an antenna is mathematically defined as the ratio of the radiation intensity of the antenna to the radiation intensity of isotropic antenna.

i.e. Directive Gain = $\frac{\psi(\theta,\Phi)}{\psi(\text{avg})} = 4\pi \cdot \frac{\psi(\theta,\Phi)}{W(\text{rad})}$

where, $\psi(\theta,\Phi)$ = radiation intensity of given antenna

$\psi(avg)$ = radiation intensity of isotropic antenna

The gain of the antenna is defined as the ratio of the intensity in a particular direction, to the radiation intensity provided by an isotropic antenna. The gain is expressed in dB

Maximum gain of antenna is as follows

$G = \eta \times D$

$\eta$ = efficiency of the antenna

D = Directivity

### 2.2.4 Scattering parameters

Scattering parameter is the most important parameter for comparison and analyzing the performance of proposed antenna. S-parameter gives the relationship between input and output ports in electrical systems. It gives the information of power reflected, impedance match, coupling between the ports, gain, correlation coefficient, directive gain.

S-Parameters

$S_{11}$ = power transfer from port 1 to port 1.

$S_{12}$ = power transfer from port 2 to port 1.

$S_{21}$ = power transfer from port 1 to port 2.

$S_{22}$ = power transfer from port 2 to port 2.

If $S_{11}$ = 0 dB then nothing is radiated all the power is reflected by the antenna,

$S_{21}$ = -10 dB then if, 1 watt is delivered to antenna 1, then 0.1 watt of power received at antenna 2.

### 2.2.5 Polarization

It is defined as "that property of an electromagnetic wave describing the time-varying direction and relative magnitude of the electric field vector, specifically, the figure traced as a function of time by the extremity of the vector at a fixed location in space, and the sense in which it is traced, as observed along the direction of propagation." Polarization is locus traced by the electric field vector tip of an electromagnetic wave. The polarization of the electromagnetic wave is characterized on the basis of its sense of rotation, axial ratio and the tilt angle. The polarization is differentiated on the basis of the linear, circular (left or right hand) and elliptical (left and right hand).

### 2.2.6 Voltage standing wave ratio (VSWR)

It measures how well antenna impedance matches with a transmission line connected to it or it a ratio of maximum voltage to minimum voltage. It is also called standing wave ratio. It is a function of the reflection coefficient. The VSWR is as shown in fig. 2.11. Mathematically, VSWR is given as

$$\text{VSWR} = \frac{1+|\Gamma|}{1-|\Gamma|} = \frac{1+S_{11}}{1-S_{11}}$$

Where $|\Gamma|$ = reflection coefficient

$1 < \text{VSWR} < \infty$

$0 < S_{11} < 1$

VSWR = 1, the antenna is perfectly matched.

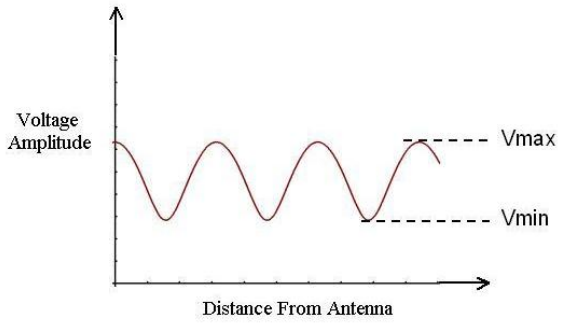


Fig. 2.11 VSWR

### 2.2.7 Input impedance

It is impedance offered by the antenna at its input terminal, or it is the ratio of electric field to magnetic field at a point or ratio of voltage to current at a pair of terminals.

Input impedance of an antenna is given by

$$Z_{in} = (R_{in} + jX_{in})$$

$R_{in}$ = it is a real part of input impedance, it represents power dissipated through radiation losses or heat.

$X_{in}$ = it is an imaginary part, it represents reactance of antenna and power stored in the near field of the antenna.

### 2.2.8 Bandwidth

The range of frequencies around center frequency which keeps the characteristics of an antenna such as beam width, polarization, gain, input impedance, radiation pattern almost close to that of this parameter. As the definition goes "the range of suitable frequencies within which the performance of the antenna, w.r.t. some characteristic, conforms to a specific standard."

Bandwidth percentage (B.W.%) = $\left[ \frac{f_H - f_L}{f_c} \right] X100$

$f_H$ = higher cut off frequency

$f_L$ = lower cut off frequency

If $\frac{f_H}{f_L}$ = 2, broadband antenna

## 2.3 Multiple Input Multiple Output (MIMO)

It is a process of increasing the channel capacity by delivering high date rate by using multiple transmitting and receiving antennas to mitigate the problem of multipath propagation[13].

MIMO antenna systems ensures good MIMO performance in terms of following parameters

- Isolation
- Envelope Correlation Coefficient(ECC)
- Total active Reflection Coefficient(TARC)
- Diversity Gain(DG)
- Multiplexing Efficiency(ME)
- Mean Effective Gain(MEG)

**2.3.1 Correlation coefficient:** To evaluate the diversity capabilities of MIMO antenna, the correlation coefficient is an important factor since lower the correlation coefficient, higher the diversity gain, and vice-versa. The correlation coefficient can be calculated from radiation pattern. The generalized expression for correlation coefficient is

$$\rho_e = \frac{(\phi(XPRE_{\theta X}(\Omega)E_{\theta Y}*(\Omega)P_\theta(\Omega)+E_{\theta X}(\Omega)E_{\theta Y}*P_\theta(\Omega))d\Omega)^2}{\phi(XPRG_{\theta X}(\Omega)P_\theta(\Omega)+G_{\varphi X}(\Omega)P_\varphi(\Omega))d\Omega X\phi(XPRG_{\theta Y}(\Omega)P_\theta(\Omega)+G_{\varphi Y}(\Omega)P_\varphi(\Omega))d\Omega}$$

Where $\Omega = (\theta, \varphi)$, $G_\theta = E_\theta(\Omega)E_\theta*(\Omega)$, $E_{\theta Y}(\Omega)$ and $E_{\theta X}*(\Omega)$ are the $\theta$ polarized complex radiation patterns of antenna Y and x in the diversity system and $d\Omega = \sin\theta d\varphi d\theta.$

$P_\varphi(\Omega)$ , $p_\theta(\Omega)$ = power spectra of incoming polarized waves.

### 2.3.2 Mean effective gain (MEG):

The power received by the antenna in a multipath environment. For the best antenna design, MEG values should be equal for all antennas. Its characteristic includes antenna efficiency, power pattern and propagation effects. The expression for MEG is given by

$$MEG = \int_0^{2\Pi}\int_0^{2\Pi}\left(\frac{XPR}{XPR+1}G_\theta(\theta,\phi)P_\theta(\theta,\phi)+\frac{1}{XPR+1}G\varphi(\theta,\varphi)P_\varphi(\theta,\varphi)\right)\sin\theta d\varphi d\theta$$

$p_\varphi$ , $p_\theta$ = angular density function of the incident power

$G_\varphi, G_\theta$ = gain pattern of the antenna at $\varphi$ and $\theta$ polarizations.

### 2.3.3 Total active reflection coefficient (TARC):

It is the ratio of the square root of total reflected power to the square root of the incident power. The TARC at the M port antenna is given by

$$\Gamma_a^t = \frac{\sqrt{\sum_{i=1}^{M}|b_i|^2}}{\sqrt{\sum_{i=1}^{M}|a_i|^2}}$$

### 2.3.4 Isolation:

It evaluates how tightly coupled antennas are. For example, the isolation between smartphone GPS and wifi antenna are of the order of 20-30 dB. Isolation of higher order is preferred.

The following mechanisms enhance the isolation:

- Adjacent antenna with different polarization
- Increasing physical spacing between antennas
- Reducing the correlation coefficient between the antennas

### 2.3.5 Multiplexing Efficiency (ME):

It shows the loss of power efficiency when using multiple antennae to achieve same channel capacity as that of the ideal array configuration in the same propagation wireless channel.

ME for two array prototype, $\eta_{mux} = \sqrt{(\eta_1\eta_2(1-|\Gamma|^2))}$

$\eta_i$ = total efficiency of antenna i

$|\Gamma|$ = complex correlation

### 2.3.6 Diversity gain (DG):

Without performance loss how much transmission power is reduced by using diversity schemes and the increase in signal to noise ratio is called as diversity gain.

## 2.4 Software tool

There are a number of software tools present in the market for analysis of antenna characteristics. Basically, these software are based on the method of analysis as discussed in above section. Some of them are CST Microwave studio, HFSS, IE3D, FEKO, etc. in this project CST studio [14] is used for analysis of patch antenna. So, some features of CST Microwave is discussed below.

CST Microwave Studio is a software tool for the three-dimensional electromagnetic simulation of high frequency components. CST provides fast and accurate analysis of high frequency devices such as antennas, MIMO antennas, filters, planar and multi-layer structure. Basically CST is user-friendly and it gives a quick EM behavior of any high frequency design.

CST provides a variety of solver technology which gives great flexibility in tackling a variety of applications. Gerenerally, CST provides Time Domain solver and The Frequency Domain Solver while CST MWS offers further solver modules for the specific application. CST MWS is much used in various industries because of its high standards.

As described earlier CST is user-friendly, thus it is quite easy to use and fully automatic i.e. it performs all mathematically calculation in background processing. Newly added features such as Optimisation strategies allow optimization even for multiple parameters within a stipulated time-bound limits.

CST Microwave Studio provides its powerful solver modules and technology leading to time domain solver, modules based on methods of analysis such as FEM, MoM, MLFMM is available which offers distinct advantages in their own domains, enables user for unprecedented simulation reliability through cross verification. These solvers are listed below:

- Resonant solver
- Transient solver
- Asymptotic solver
- Eigen mode solver
- Frequency domain solver
- Integral equation solver

## 2.5 Literature Survey

### 2.5.1 Introduction

Prior to starting of my thesis, it is important to have a deep understanding of previous research work on microstrip patch antenna isolation at millimeter wave for the future 5G wireless application. The main sources of information for dissertation are books, journals, magazines, thesis, dissertations and the internet. This chapter covers the research paper review.

### 2.5.2 Literature paper review

In order to start thesis work, the first thing is to study previous research papers that have been performed by previous researchers. Research papers related to this work is chosen and studied**.**

A compact slotted planar square ring-shaped microstrip antenna simultaneously suitable for point to point communication at 60 GHz [15]. The antenna is simulated by

the software CST. CST, computer simulated technology simulator is employed to analyze the proposed antenna, and simulated results on return loss, the E and H-plane radiation pattern and polar plot gain are presented. The simulation and measurement result met the IEEE 802.l1ad standard operate in 60 GHz band for point to point communication. The measured results show a return loss of -26.69 dB and the voltage standing wave ratio VSWR < 2 at 60 GHz indicating that the antenna is a good candidate for very high-speed WLAN applications.

A new dielectric resonator antenna (DRA) for a millimeter-wave (mm-wave) multiple-input–multiple-output system is discussed in [16]. Two approaches are exploited to reduce the mutual coupling between two antenna elements. First, a frequency selective surface (FSS) wall is inserted between the DRAs to reduce the free-space radiation. Then, two slots with different size acting like an LC resonator are etched from the common ground plane of the structure to reduce the surface current. The designed FSS has a wideband characteristic from 40 to 70 GHz. The FSS is optimized for the desired frequency of 57–63 GHz. A high isolation of −30 dB is achieved when both FSS wall and slots are used. A prototype of the structure is fabricated and measured. The results give a low correlation coefficient (< 5e-6) and a good agreement with simulation ones, indicating that the proposed antenna can provide spatial or pattern diversity to increase the data capacity of wireless communication systems at mm-wave bands.

The proposed antenna consists of a 2-port octangular patch antenna and a 2-port square ring antenna constituting a 4 element MIMO antenna [17]. The isolation is achieved here by etching twelve slots on the ground at the strong coupling areas. The proposed isolation structure reduces surface waves confined within the dielectric that causes coupling between antenna elements. Isolation is improved by 10 dB. The antenna operates with 50 MHz bandwidth centered at 2.44 GHz and also correlation coefficient is below 0.1, which satisfy good MIMO performance.

In order to enhance the isolation, a new technique is discussed [18], asymmetrical coplanar strip (ACPS) wall to suppress the mutual coupling between two closely spaced 5.8 GHz microstrip antennas. The ACPS wall, which is inserted vertically between the two antennas, introduces an additional coupling path to reduce the antenna coupling, occupying just a small area between the two antennas. The decoupling effect of the proposed structure is verified by the simulation and

measurement. The experimental results show that the achieved isolation is better than 35 dB and reaches a maximum of 54.3 dB at 5.8 GHz, with an extremely close antenna distance of (edge-to-edge distance). The measured patterns indicate that the proposed structure also improves the radiation of the microstrip antenna.

A review of various MIMO antenna isolation techniques such as decoupling networks, defected ground structures, Neutralization line, parasitic elements and metamaterials are discussed [19]. From the given isolation techniques defected ground structures, decoupling networks and metamaterials are better than the remaining techniques.

The source of mutual coupling is first identified and, accordingly, the appropriate isolator is designed [20]. The main source of mutual coupling is surface waves and space waves taken into consideration. The isolator consists of a piece of mushroom-like EBG structure that has been placed inside a metallic choke. This structure is placed between two metallic walls which are lying between two microstrip patch antenna. It increases the isolation more than the 40 dB at the cost of reducing matching bandwidth.

A new approach to improve isolation between microstrip patch antenna arrays is realized by creating a defect in microstrip patch structure called SLMR [21] in between array at 4.8 GHz. The SMLR resonator blocks the surface current at operating frequency. The fundamental resonant frequency of band rejects filter is controlled by the length of the slot in structure. And results compared to remaining isolation techniques. The improvement in isolation is 16dB with an edge to edge spacing of λ/9. The simulations are carried out using CST software.

The proposed patch for six different substrate permittivity height and length are discussed at 60GHz [22]. The parameters discussed are the VSWR, return loss, gain, directivity, bandwidth. The given substrates are the RT Duroid 5880, Arlon Diclad 522, Teflon, Bakelite, Dupont 951, Teconic RF 35P. Among the following, Arlon Diclad 522 is the better substrate.

Three split ring resonator cell is demonstrated [23]. Split ring resonator metamaterial acts as a LC resonant tank. The length and the spacing between the 3-split ring resonator are optimized and the array placed between the microstrip patch antenna. The conductive element in metamaterial creates the inductive effect, and the gap

between the ring creates the capacitive effect. The isolation at 9.6 GHz is -23 dB. There is a reduction of 5db in mutual coupling at the resonant frequency.

The three interdigital lines excite the orthogonal polarization mode in adjacent patch antenna in order to reduce the mutual coupling [24]. The current distribution and electric field reveal the mechanism of the structure. The length of the three interdigital lines is optimized and placed between the patch. The experimental results show the maximum isolation enhancement of -24 dB with an edge to edge separation of 0.07λ.

To mitigate the problem of mutual coupling UC-EBG structures placed on top of the radiating antenna layer instead of mushroom-like EBG structure [25]. By changing the geometrical dimensions of each unit cell, the frequency band gap of the UC-EBG structure can be tuned. About 10 dB and 14 dB reduction in mutual coupling occurred by using two rows and three rows of UC-EBG superstrate respectively. And the separation distance between radiating patch is reduced from 0.63λ to 0.5λ.

Instead of the conventional substrate, the antenna array built on metamaterial substrate which shows significant size reduction and reduced mutual coupling [26]. This antenna has high gain, omnidirectional radiation pattern and very good pattern stability over operating band (5.1- 5.9 GHz). It covers the IEEE 802.11a (5.15-5.35 GHz and 5.47-5.725 GHz) American Standards and HIPPER LAN/2 (5.15-5.35 GHz and 5.725-5.825 GHz) European standard. The mutual coupling has been reduced by about 12–19 dB at all frequencies (5.1–5.9 GHz), while maintaining good impedance matching for the two-antenna system by using metamaterial substrate and the Elliptical SRRs array separation between the antenna elements. The increase in isolation of about 19dB occurs at the operating bandwidth.

The design of a small-size ($48\times48\ mm^2$) MIMO antenna system with low mutual coupling for LTE 800 MHz applications [27]. The antenna system comprises of two FR-4 substrate layers; one printed with two meander line antennas (MLAs), the other printed with reactive impedance surface (RIS) and defected ground structure (DGS). The properties of the antenna like S-Parameters, excited surface current distribution, far-field radiation pattern and diversity performance characteristics were studied. The introduction of the air gap (AG) between the two substrates, DGS and periodic square patches of RIS resulted in 452 MHz bandwidth and mutual coupling of −41.18 dB

between antenna elements. Parameters including bandwidth, the ratio of antenna area/improvement in $S_{12}$, antenna efficiency and the envelope correlation coefficient were compared.

A multi-input-multi-output (MIMO) antenna with improved isolation using an interdigital split ring resonator (SRR) is proposed [28]. The necessary impedance bandwidth is obtained by utilizing the coupling between the meander strip and an inverted L strip. Using interdigital SRR, a negative permeability was generated, while achieving improved isolation between the two radiating elements. The fabricated antenna satisfies the 10 dB return loss in the long-term evolution (LTE) band 40 from 2.3 GHz to 2.4 GHz. The measured peak gains of the two elements were 1.3 dBi and 2.0 dBi. The measured envelope correlation coefficient was less than 0.16 over the frequency band of interest.

A very compact ultrawideband (UWB) multiple-input multiple-output (MIMO) antenna with high isolation [29] is analyzed. The overall dimension of proposed antenna is $22 \times 26$ mm$^2$. To improve isolation, two defected ground structure is utilized. The T-shaped slot is etched on the ground contribute two functions, reducing surface current and extending the current path length, enhances the isolation at the band 4–10.6 GHz. To improve isolation at the band 3-4 GHz, a line slot etched on the ground which brings new coupling cancels the original coupling. The antenna shows the mutual coupling less than -18 dB at operating band 3.1-10.6 GHz.

Another compact ultrawideband (UWB) MIMO antenna with a very low mutual coupling covering 2.4 GHz WLAN and 3.1–10.6 GHz UWB bands is proposed [30]. The proposed antenna is based on meandering monopoles; an ultrawide bandwidth is achieved by involving two smaller L-shape stubs and two inverted L-shape parasitic strips, and by etching a slot at the center of the ground, a high isolation is obtained. The prototype design is simulated, fabricated, and measured. A good agreement between the measured and simulated results shows that an ultrawide bandwidth and a high isolation are successfully achieved.

The development of a miniaturized two-element printed MIMO antenna with high isolation and improved radiation efficiency by using metamaterial configuration for triple band operation frequencies: (2.4-2.485) GHz, (5.1-5.35) GHz for Wi-Fi and (3.35-3.8) GHz for Wi-Max [31]. The two patch antenna printed on FR-4 substrate

with overall dimension 40 × 27.2 $mm^2$ is designed, simulated and fabricated. The proposed antenna uses three geometrical configuration to meet above goal. Firstly, for introducing triple band operation split-ring resonator(SRR) is introduced in patch. Secondly, improving isolation between patch antennas neutralization lines are incorporated. Finally, to improve further in terms of isolation and radiation efficiency it incorporates a double-sided metamaterial grid.

A compact planar T- slotted microstrip antenna suitable for 5G Wireless communication at millimeter wave frequency [32] is proposed. The simulation result met the IEEE 802.11ad standard operating in 60 GHz millimeter wave frequency band suitable for 5G Wireless communication. The measured results show the lowest return loss of -38 dB, gain of the antenna is 6.34 dB and the voltage standing wave ratio (VSWR) is near to 1 at 23 GHz and 60 GHz indicating that the antenna is a good candidate for very high-speed WLAN applications.

The antenna array with a U-shape neutralization line entrenched for hepta-band WWAN/LTE operation in the smartphone applications is studied and presented [33]. By placing the U-shape neutralization line, the isolation in between the antenna elements is significantly enhanced for the lower band, with no undesirable effects on the upper band. The antenna covers the operating hepta band: GSM850/900/1800/1900/UMTS/LTE2300/2500 with mutual coupling less than -10.5 dB. The measured results of radiation efficiencies, s-parameter, 3-D radiation patterns, mean effective gain (MEGs), and envelope correlation coefficient (ECCs) are presented and can meet the requirements of multiantenna systems.

In this paper, a novel 60-GHz antenna based on the complementary source technique for circular polarization application is designed [34]. The proposed antenna is composed of a slot, a strip dipole, and a cavity, and it is realized by plated through hole and printed circuit technologies. The results show that the proposed antenna covers the overlapping bandwidth of 21.9% from 53.6 to 66.8 GHz which includes the whole 60 GHz band. The radiation pattern of experiments and simulation are almost same.

# CHAPTER-3

# PROPOSED DESIGN OF MIMO ANTENNA AT 60 GHZ BAND USING ISOLATION TECHNIQUES

## 3.1 Introduction

In this thesis, the effect of mutual coupling in MIMO antenna array system at millimeter wave 60 GHz for future 5G wireless communication is analyzed using CST studio. The CST software simulates the radiation pattern of given antenna array and measures the mutual coupling between them. In general, for designing and computing the results of the antenna characteristics in higher frequency, CST software is an essential numerical tool used for predicting the trend of the coupling coefficient in an antenna array. In subsequent sections, the coupling coefficient, return loss, gain, surface current, radiation pattern, efficiencies with and without isolation techniques are computed, compared and analyzed in detail.

## 3.2 Proposed design of an antenna at 60 GHz

In this work, antennas are modeled in CST Studio at a frequency 60 GHz, which gives rise to wavelength 5mm. In the simulation design, I-shaped patch antenna is designed with microstrip feed. The patch consists of length $0.86\lambda_0$ and width $1.11\lambda_0$. The antenna is constructed on RT Duroid 5880 (lossy) having dielectric constant 2.2, loss tangent 0.0009 and the height of substrate is 0.254 mm. The spacing between the microstrip patch is less than $\lambda_0/2$ . The remaining patches are lying on common substrate and share common ground plane for MIMO applications. The waveguide port is used for excitation which extends through ground to five times of substrate height. For all the simulations, the fast solver sweep scheme is used to sweep through a frequency range 55 GHz to 65 GHz. It is important to select a frequency sweep range for the fast sweep scheme in such a way that the solution frequency nearly 60 GHz lies exactly in the middle for better accuracy.

**Structure in CST**

Antenna at single 60 GHz band is designed with the following dimensions as shown in fig. 3.1 and dimensions are tabulated in table 3.1

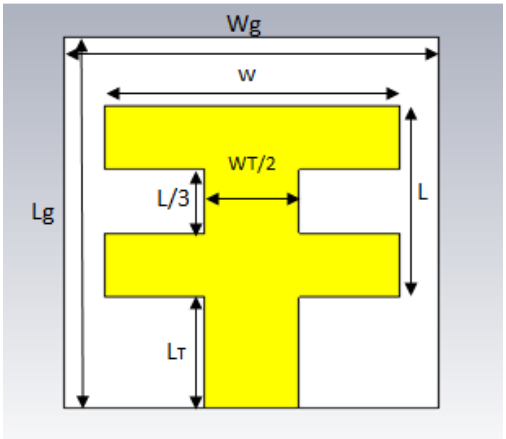


Fig. 3.1Proposed design of single I-shaped patch antenna

TABLE 3.1: The design specification of proposed I-shaped antenna

| PARAMETERS | DIMENSIONS (mm) |
|---|---|
| **Lg (Length of ground)** | 8.314 |
| **Wg (width of ground)** | 7.094 |
| **L** | 4.3 |
| **W** | 5.57 |
| **$L_T$** | 2.49 |
| **$W_T$** | 1.79 |
| **H (Height of substrate)** | 0.254 |

The simulation results of the above design have yield following antenna characteristics: return loss ($S_{11}$), VSWR and 3-D directivity view. These are shown below and discussed one by one.

The most important parameter in regards to the antenna is $S_{11}$. The return loss $S_{11}$ measures the power reflected by the antenna due to impedance mismatch. And it also

shows the frequency at which antenna resonant. Lower the return loss curve minimum the reflection from the antenna. The return loss curve is shown in fig. 3.2

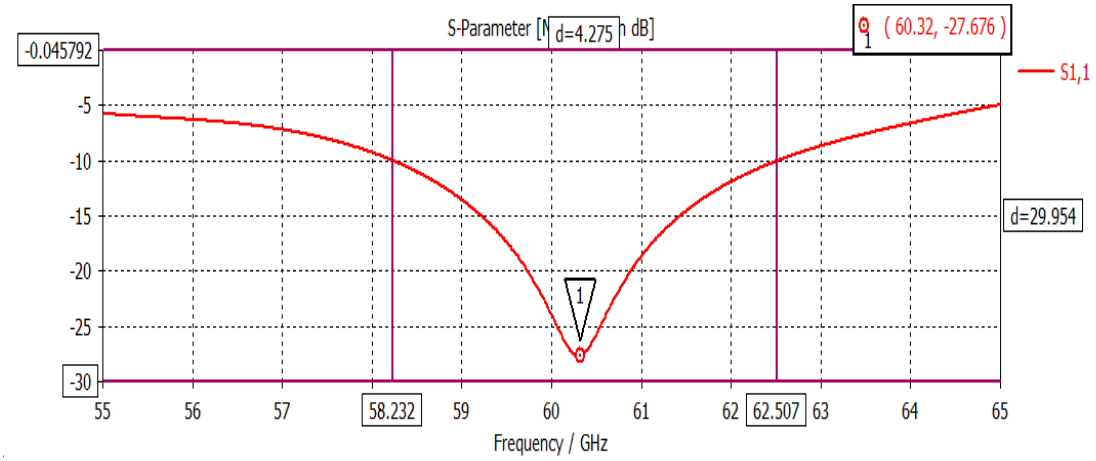


Fig. 3.2 Return loss of single band I-shaped patch antenna

From fig. 3.2, we can check the resonance frequency along with matching bandwidth. Generally, the bandwidth of consideration is seen at -10 dB return loss and for this band the reflected power is low to disturb the antenna characteristics.

Thus,

$S_{11}$ = -27.676

Resonant frequency $f_r$ = 60.32 GHz

$f_H$ = 62.507 GHz

$f_L$ = 58.232 GHz

Bandwidth = 4.275 GHz

Another important parameter comes under the picture is VSWR. It is the ratio of voltage maxima to voltage minima. Ideally, it should be 1, but practically, it should be less than 2. From fig.3.3, it is concluded that, for entire band of operation the VSWR is less than 2. Hence antenna is well matched.

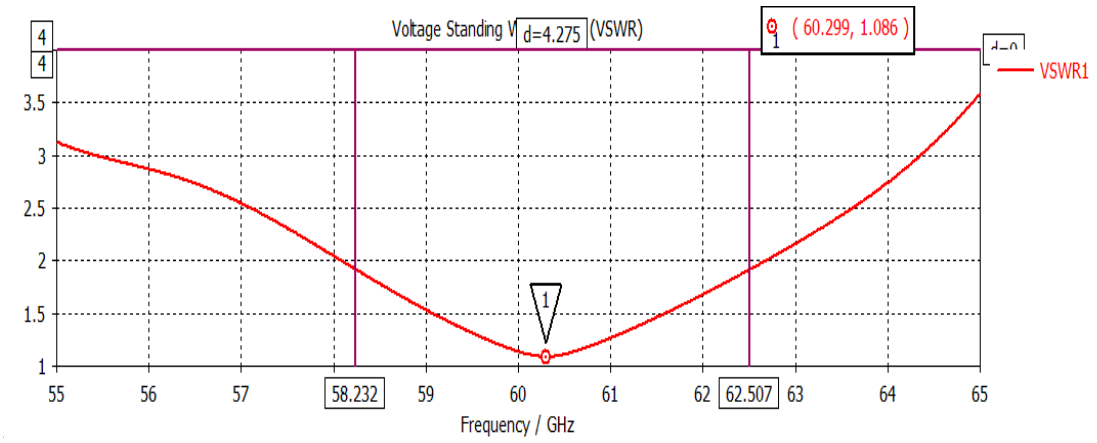


Fig. 3.3 VSWR of single band I-shaped patch antenna

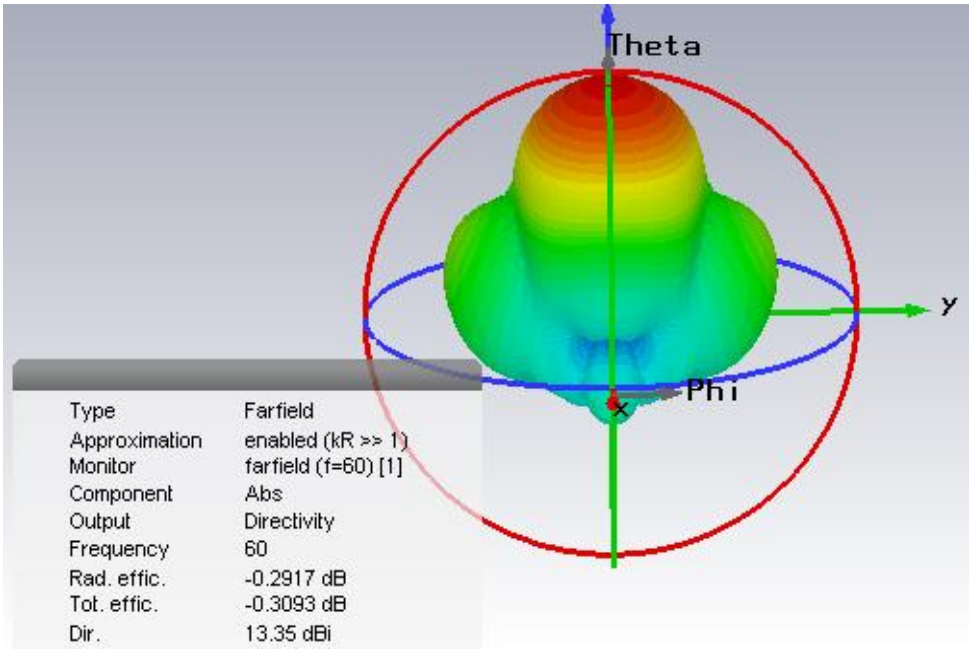


Fig. 3.4 3D Directivity plot of single band I-shaped patch antenna

From the directivity curve as shown in fig. 3.4, it is clear that majority of the power of given antenna radiates its power towards the main lobe with directivity i.e. maximum gain of 13.35 dBi.

## 3.3 Proposed design of I-shaped patch antenna with slot cut in upper arm

The same antenna with slot cut of length $\lambda_0/4$ in the middle of upper arm of I-shaped patch antenna shows better antenna characteristics as compare to without slot, with

slot of different length $\lambda_0$, $\lambda_0/2$, $\lambda_0/8$. The microstrip patch antenna given in fig. 3.5 shows slot cut of $\lambda_0/4$. The width of the slot is 0.02 mm.

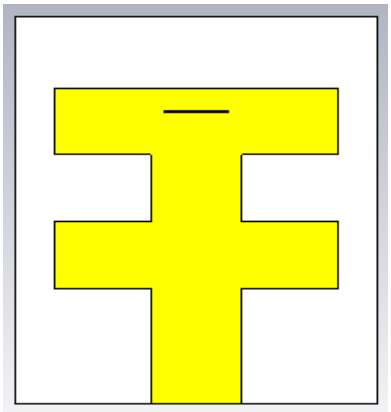

Fig. 3.5 Proposed design of antenna with $\lambda_0/4$ slot in patch

Antenna characteristics of above structure of slot length $\lambda_0/8$, $\lambda_0/4$ , $\lambda_0/2$, $\lambda_0$ is simulated for analysis of slot effect on antenna. The fruitful result is coming only for slot length $\lambda_0/4$. The antenna characteristics are shown in fig.3.6, fig.3.7 and fig.3.8 for slot $\lambda_0/4$.

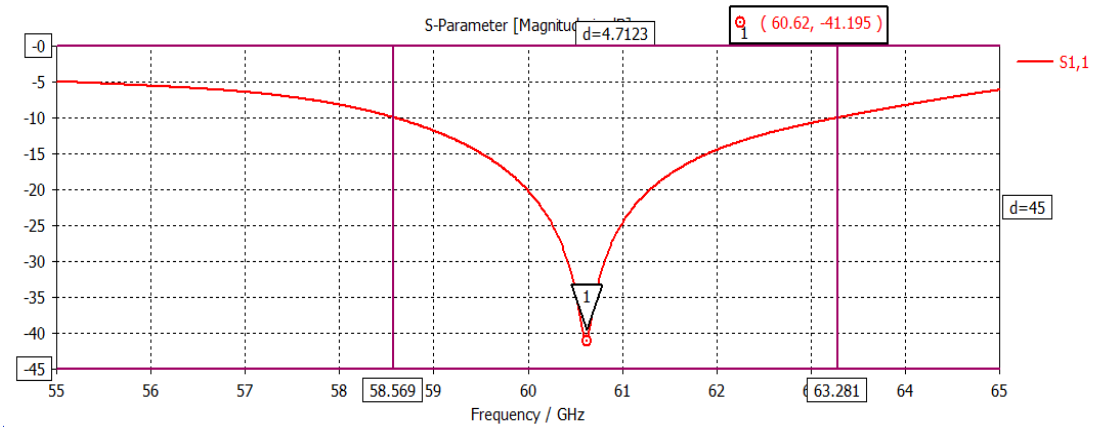


Fig. 3.6 Return loss of an antenna with $\lambda_0/4$ slot in upper arm of I-shaped patch.

From fig. 3.6 and fig. 3.7 we observe that $S_{11}$ = -41.195, resonant frequency $f_r$ = 60.62GHz, $f_H$ = 62.281 GHz , $f_L$ = 58.569 GHz and bandwidth = 4.7123 GHz and VSWR less than 2.

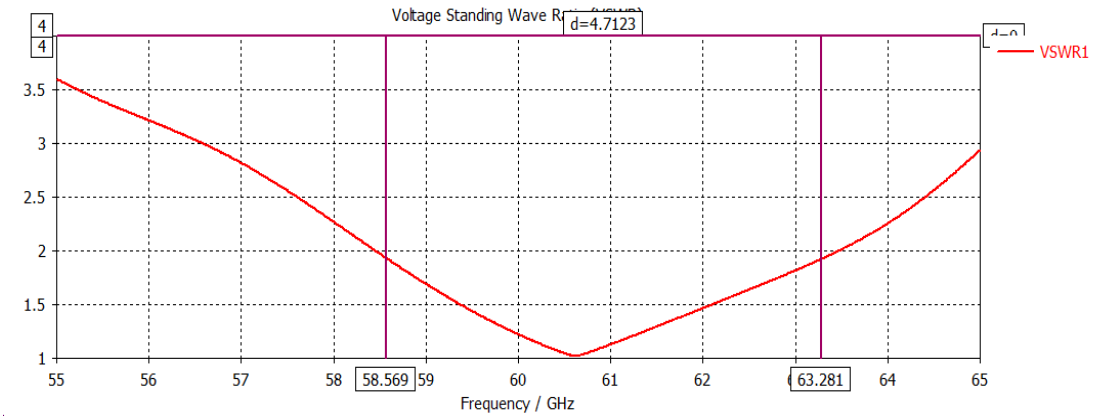


Fig. 3.7 VSWR of an antenna with $\lambda_0/4$ slot in upper arm of I-shaped patch

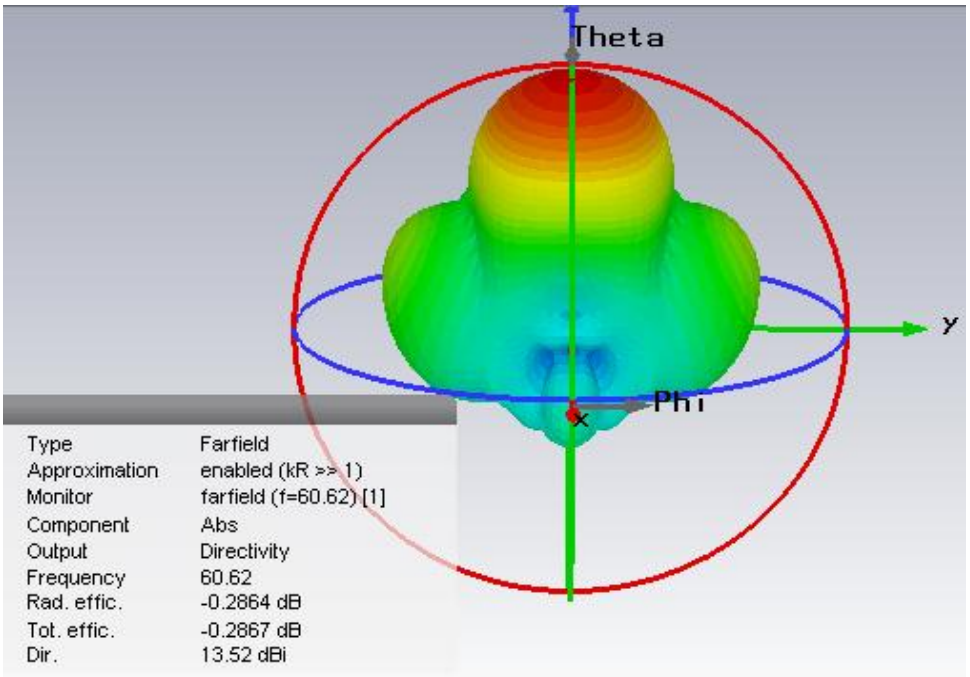


Fig. 3.8 3D directivity plot of an antenna with $\lambda_0/4$ slot in upper arm of I-shaped patch

The directivity of the antenna increases with introducing slot in upper arm. The directivity is 13.52 dBi as depicted in fig. 3.8. Comparison between microstrip patch antenna with and without a slot in I-shaped patch antenna is tabulated in Table 3.2 and conclusions are drawn from the above performed simulations.

TABLE 3.2 Comparison between without slot, with slot length $\lambda_0/4$ and $\lambda_0/8$

| **PARAMETERS** | **Without slot** | **With Slot $\lambda_0/4$** | **With slot $\lambda_0/8$** |
|---|---|---|---|
| **Resonant frequency(GHz)** | 60.32 | 60.62 | 60.527 |
| **Bandwidth (GHz)** | 4.275 | 4.7123 | 4.331 |
| **Gain (dB)** | 13.5 | 13.52 | 13 |
| **Return loss** | -27.676 | -41.195 | -23.691 |

From the above table 3.2, it is concluded that the

- Antenna with slot length $\lambda_0$and $\lambda_0/2$ are showing return loss higher than -10 dB hence, they are not taken under consideration of designing and analyzing further.
- Antenna with $\lambda_0/4$ has matching bandwidth 4.7123 GHz which is more than the bandwidth of without slot, with slot $\lambda_0/8$, $\lambda_0$ and $\lambda_0/2$.
- Return loss with slot $\lambda_0/4$ is less than the remaining slots and without slot.
- Gain of the antenna with slot $\lambda_0/4$ is more than the remaining slots and without slot.

The proposed structure is examined for different slot length, and without slot of antenna. It analyzed from the given data, that the slot length with $\lambda_0/4$ gives better results than others. Hence $\lambda_0/4$ will be optimum length for MIMO antenna.

## 3.4 Analysis of varying slot width U and L.

In this section the proposed structure is analyzed for varying upper arm and lower arm width of I-shaped patch antenna denoted by U and L, respectively. This design is depicted in fig. 3.9.

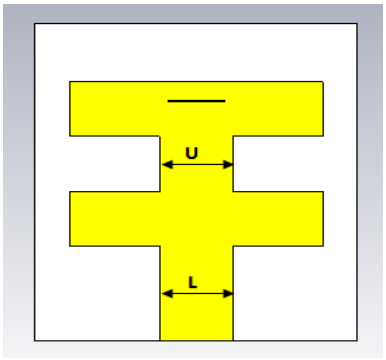


Fig. 3.9 Proposed design of antenna with dimension vary of U and L

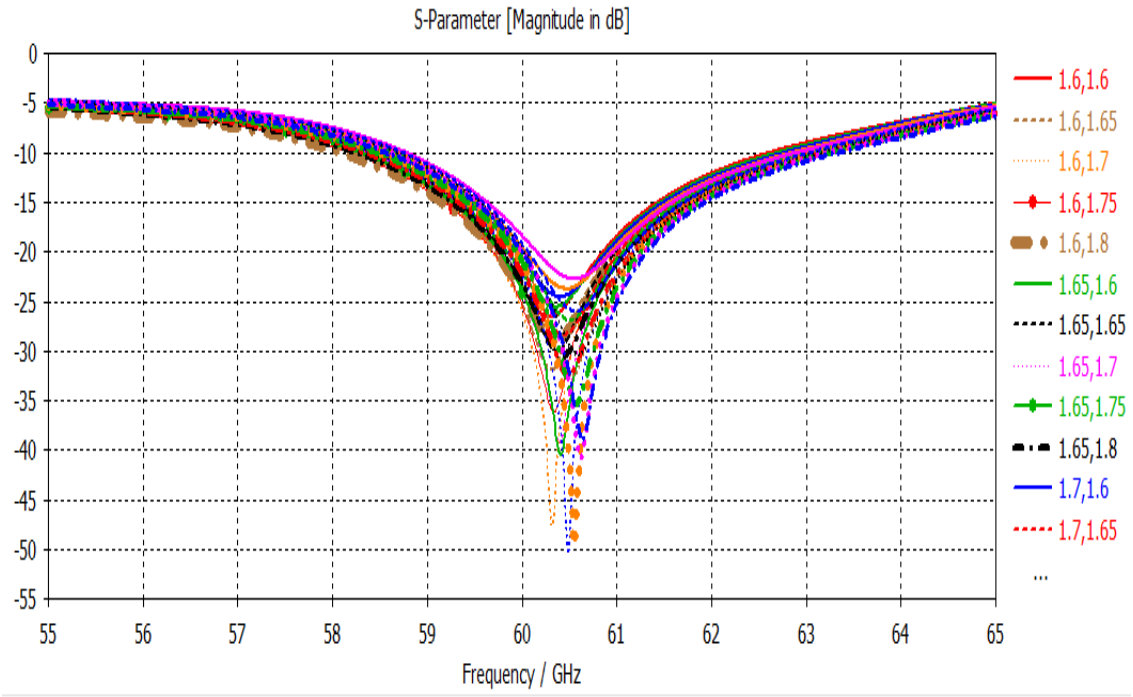


Fig. 3.10 Return loss of parameter variation U and L

From fig. 3.10, it can seen that by varying U and L there will be a change in reflection coefficient, matching bandwidth, resonant frequency, radiation pattern, etc. the impact of varying U and L is tabulated in table 3.3.

TABLE 3.3 Impact on antenna characteristics by variation of U and L

| U(mm) | L (mm) | Resonant frequency (GHz) | $S_{11}$ (dB) | Bandwidth (GHz) | Frequency range (GHz) |
|---|---|---|---|---|---|
| 1.6 | 1.6 | 60.31 | -26.589 | 4.2862 | 58.333- 62.62 |
| 1.65 | 1.6 | 60.357 | -25.565 | 4.2526 | 58.457- 62.709 |
| 1.7 | 1.6 | 60.42 | -24.516 | 5.5755 | 57.975-63.55 |
| 1.75 | 1.6 | 60.499 | -23.707 | 5.6203 | 58.042-63.662 |
| 1.8 | 1.6 | 60.576 | -22.715 | 5.59 | 58.176-63.774 |
| 1.6 | 1.65 | 60.31 | -31.933 | 4.4768 | 58.288-62.705 |
| 1.65 | 1.65 | 60.37 | -29.999 | 4.4096 | 58.401-62.81 |
| 1.7 | 1.65 | 60.44 | -28.367 | 4.3759 | 58.501-62.877 |
| 1.75 | 1.65 | 60.52 | -26.88 | 4.3199 | 58.625-62.945 |
| 1.8 | 1.65 | 60.57 | -26.002 | 4.2975 | 58.714-63.012 |
| 1.6 | 1.7 | 60.32 | -47.69 | 4.6002 | 58.247-62.799 |
| 1.65 | 1.7 | 60.4 | -39.145 | 4.588 | 58.322-62.911 |
| 1.7 | 1.7 | 60.47 | -34.971 | 4.5329 | 58.423-62.956 |
| 1.75 | 1.7 | 60.53 | -32.517 | 4.488 | 58.546-63.034 |
| 1.8 | 1.7 | 60.586 | -30.373 | 4.4656 | 58.614-63.076 |
| 1.6 | 1.75 | 60.345 | -36.094 | 4.7683 | 58.188-62.956 |
| 1.65 | 1.75 | 60.41 | -40.442 | 4.701 | 58.288-62.99 |
| 1.7 | 1.75 | 60.49 | -50.319 | 4.6674 | 58.33-63.001 |
| 1.75 | 1.75 | 60.55 | -49.617 | 4.5777 | 58.501-63.079 |
| 1.8 | 1.75 | 60.62 | -40.883 | 4.5771 | 58.602-63.18 |
| 1.6 | 1.8 | 60.373 | -28.993 | 4.8132 | 58.143-62.956 |
| 1.65 | 1.8 | 60.44 | -30.539 | 4.7235 | 58.266-62.99 |
| 1.7 | 1.8 | 60.505 | -32.379 | 4.7459 | 58.356-63.012 |
| 1.75 | 1.8 | 60.58 | -35.252 | 4.7577 | 58.445-63.203 |
| 1.8 | 1.8 | 60.64 | -38.967 | 4.6898 | 53.591-63.281 |

Following conclusions are demonstrated from table 3.3:

- For U = 1.7 and L = 1.75 gives lowest return loss from the other dimension of U and L.
- For L = 1.6, 1.65, 1.7 and by increasing U leads to
  - Shift of resonant frequency towards right
  - Return loss increases
  - Bandwidth decreases
- For L = 1.75 and 1.8 and by increasing U leads to
  - Shift of resonant frequency towards right
  - Return loss first decreases and then increases in case of L = 1.75 and return loss decreases for L = 1.8
  - Bandwidth decreases.

By analyzing the design of the single I-shaped patch antenna which resonant at desired 60 GHz band gives better radiation pattern and we use this antenna for designing of MIMO antenna arrays which is used in 5G wireless application. In the later sections, it covers the MIMO antenna array with isolation and without isolation also the impact of mutual coupling is computed and analyzed.

MIMO communication technology is implemented using multiple antennas at the transmitter side and receiver side for enhancement of channel capacity to provide higher data rate without the need of additional power. Due to competition in the market, the key parameter requirements in portable devices are the size miniaturization.

When multiple antennas are closely packed into limited space less than $\lambda/2$, the mutual coupling occurs which reduces the gain of the antenna, bandwidth, increases the surface current, degrade the radiation performance, and power absorbed by near by antenna,. To improve the isolation between the antennas different techniques developed in the past.

To improve the isolation between the antenna array, slotted meander line resonator (SMLR) and meta-materials are used.

## 3.5 Proposed antenna array design for spacing more than $\lambda_0/2$

Antenna array with spacing more than $\lambda_0/2$ is shown in fig. 3.11. The spacing more than $\lambda_0/2$ leads to less mutual coupling. So, antenna characteristics are not distrubed by neighbour antennas.

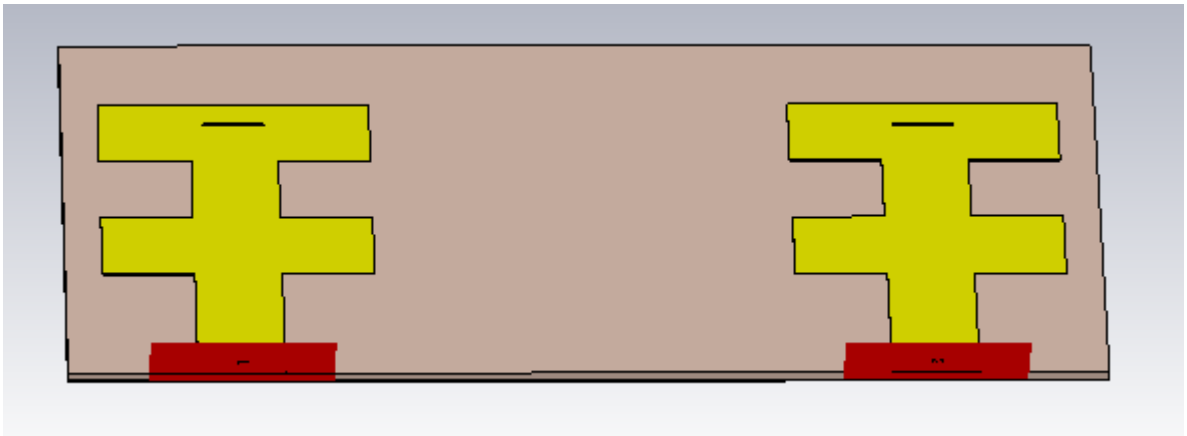

Fig. 3.11 Proposed design of an antenna array with spacing between them greater than $\lambda_0/2$

MIMO antenna array is designed as shown in fig. 3.11 with same substrate, same patch dimension as used in section 3.4 with spacing more than λ between antenna 1 and 2.

The antenna characteristics for MIMO application is computed with spacing greater than $\lambda_0$. Now the effect of mutual coupling is analyzed with help of CST Studio simulations. By simulating the design in CST Studio following results have been observed such as return loss, transmission coefficient, VSWR, radiation pattern, surface current, envelope correlation coefficient and diversity gain.

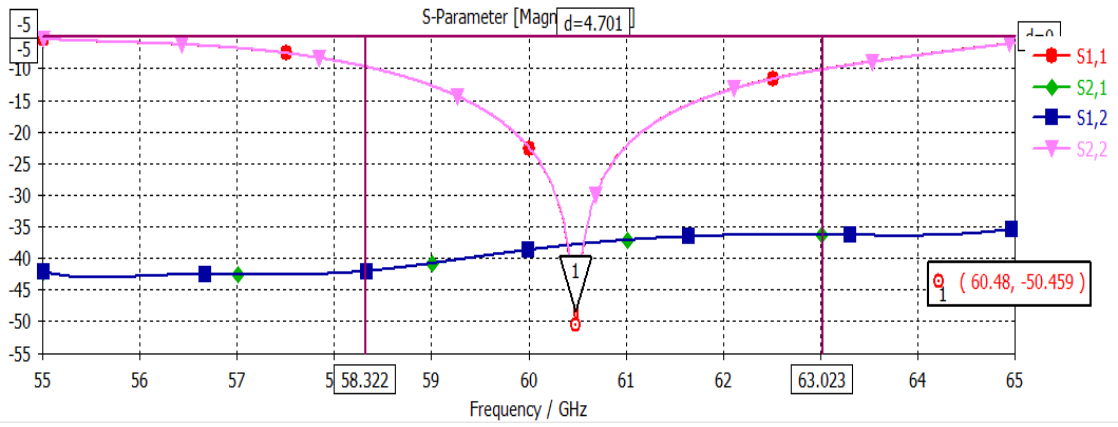


Fig. 3.12 Reflection and transmission coefficient of an antenna with spacing greater than $\lambda_0$.

Transmission coefficient ($s_{12}, s_{21}$) shows the power transfer from one antenna to neighbour antenna. The curve shown in fig. 3.12 shows the transmission coefficient and reflection coefficient. As $S_{11}$, $S_{12}$, $S_{21}$ and $S_{22}$ reduces, antenna characteristics get improves. Lowering of S-parameters implies less power is transfer from antenna 1 to 2 or vice-versa, and also less reflections take place. From fig. 3.12 the VSWR is less than 2 in desired 60 GHz band which shows the matching is best between patch antenna and microstrip feed line.

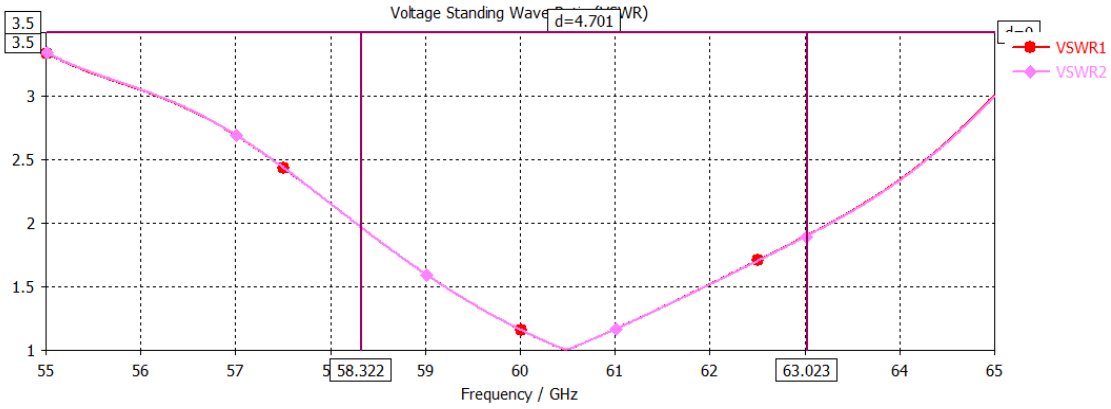


Fig. 3.13 VSWR of an antenna array with spacing more than $\lambda_0$

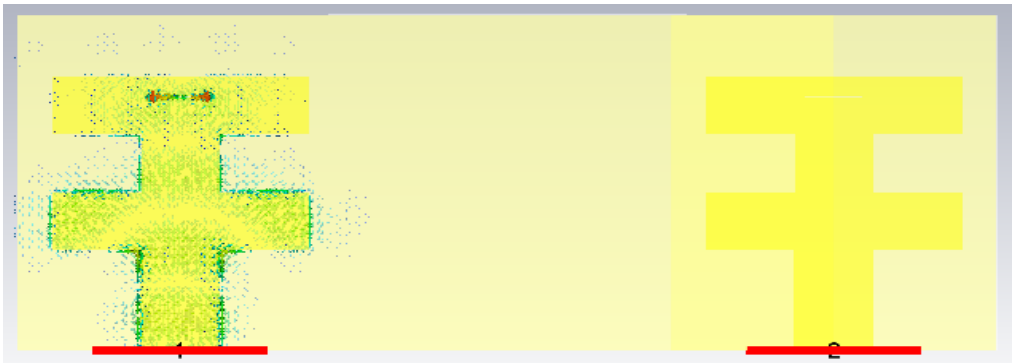

Fig. 3.14 Surface current at 60 GHz with spacing more than $\lambda_0$

For proper radiation of antenna the oscillating surface current from antenna 1 to 2 should be minimum. The surface current distribution of the configuration (fig. 3.11) is depicted in fig. 3.14. From the following fig. 3.14, the surface current of antenna 1 is not oscillating to antenna 2.

The main sources of electromagnetic coupling in the antenna array is conducting current due to continous ground plane, surface waves due to continous dielectric substrate, and radiated space wave in free space. When antenna elements are placed on different grounded dielectric shows minimum mutual coupling rather than on common grounded dielectric. The level of mutual coupling depends on dielectric constant of substrate and distance between radiating elements.

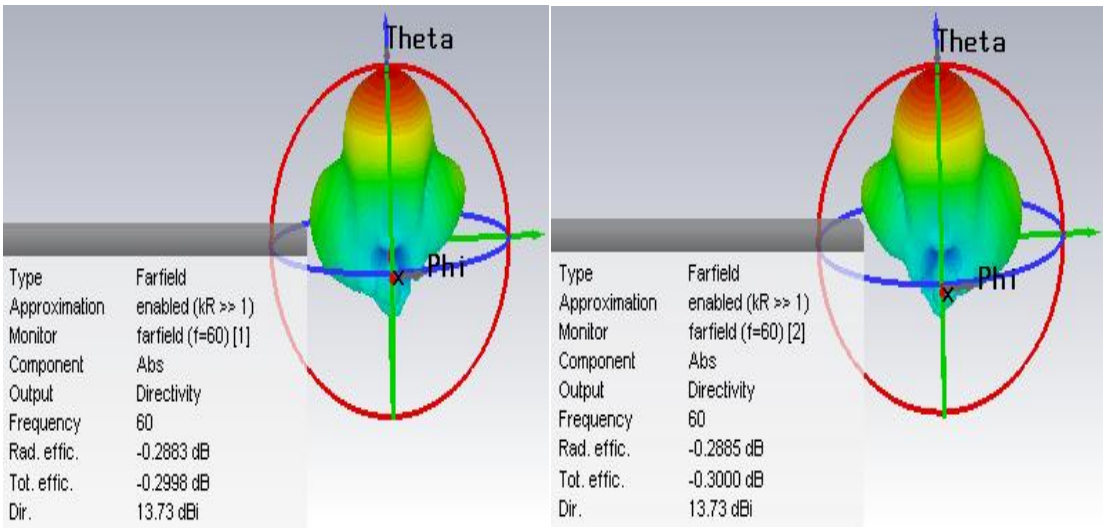


a) Antenna 1 b) Antenna 2

Fig. 3.15 3D directivity plot of an antenna a) and b) with spacing more than $\lambda_0$

The 3D directivity pattern of antenna 1 and 2 is depicted in fig. 3.15. The directivity of antenna 1 and 2 is 13.73 dBi.

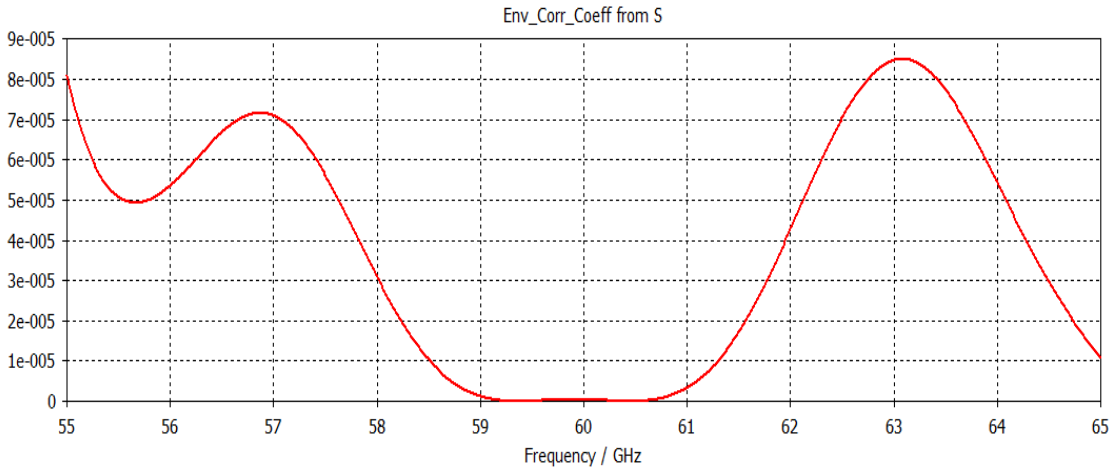


Fig. 3.16 Envelope correlation coefficient between antenna 1 and 2 with spacing more than $\lambda_0$

From the fig. 3.16, the correlation coefficient is less than 3e-005, hence antennas are very less correlated. It has been demonstrated that the characteristics of antenna 2 is not disturbed by the antenna 1. The diversity gain of antenna 1 and 2 is shown in fig. 3.17.

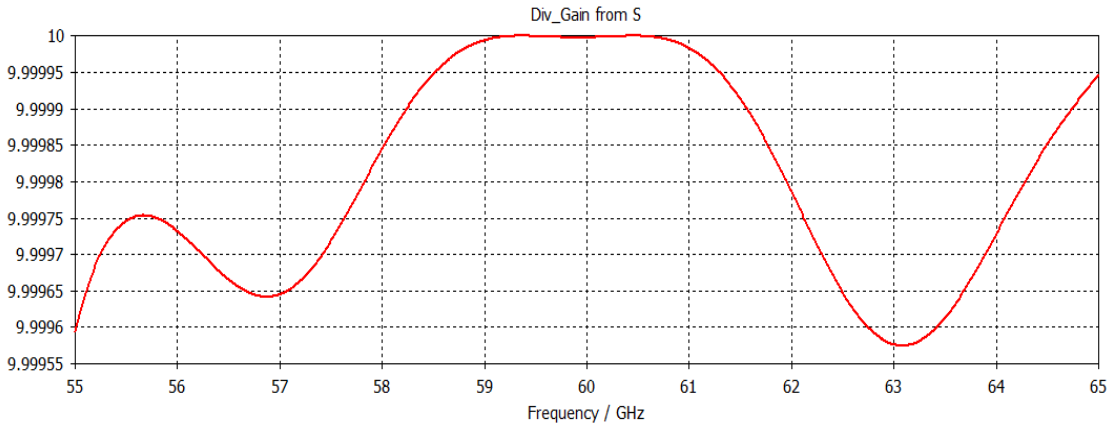


Fig.3.17 Diversity gain of antenna 1 and 2 with spacing more than $\lambda_0$

## 3.6 Proposed antenna array design for spacing less than $\lambda_0/2$

Antenna array with spacing less than $\lambda_0/2$ i.e. 1.524mm is shown in fig. 4.7 which causes mutual coupling and degrades the performance of MIMO antenna array.

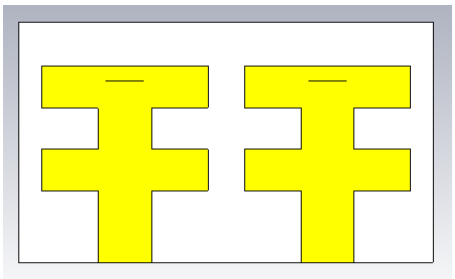

Fig. 3.18 MIMO antenna array with spacing less than $\lambda_0/2$

Now the results are analyzed for spacing less than $\lambda_0/2$

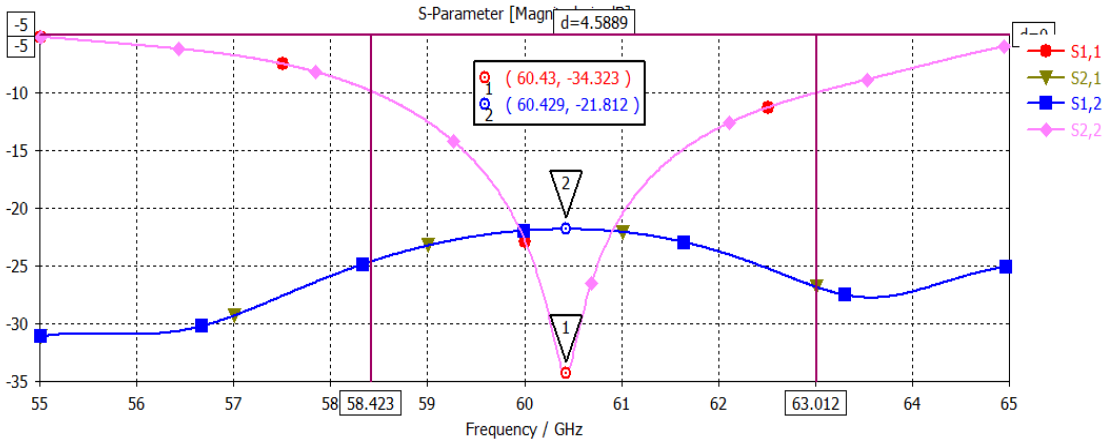


Fig. 3.19 Reflection and transmission coefficient of antenna 1 and 2 with spacing less than $\lambda_0/2$

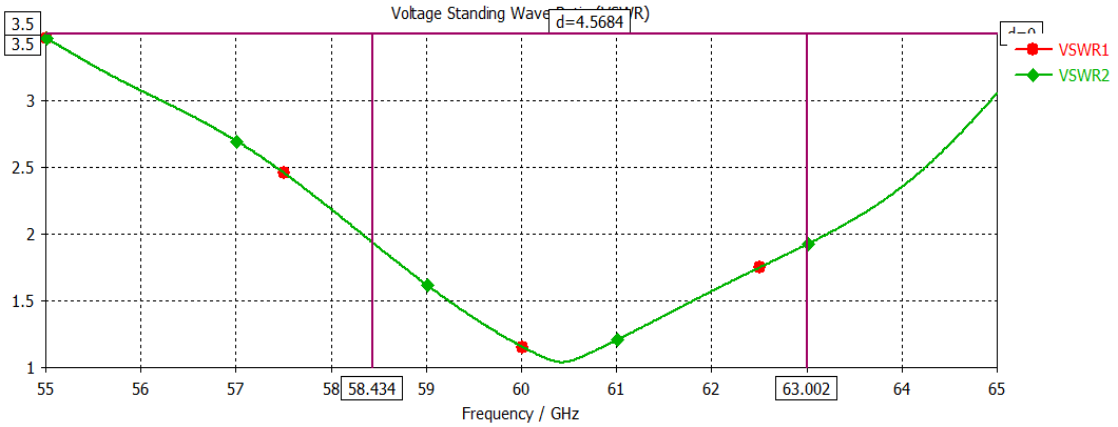


Fig. 3.20 VSWR of antenna 1 and 2 with spacing less than $\lambda_0/2$

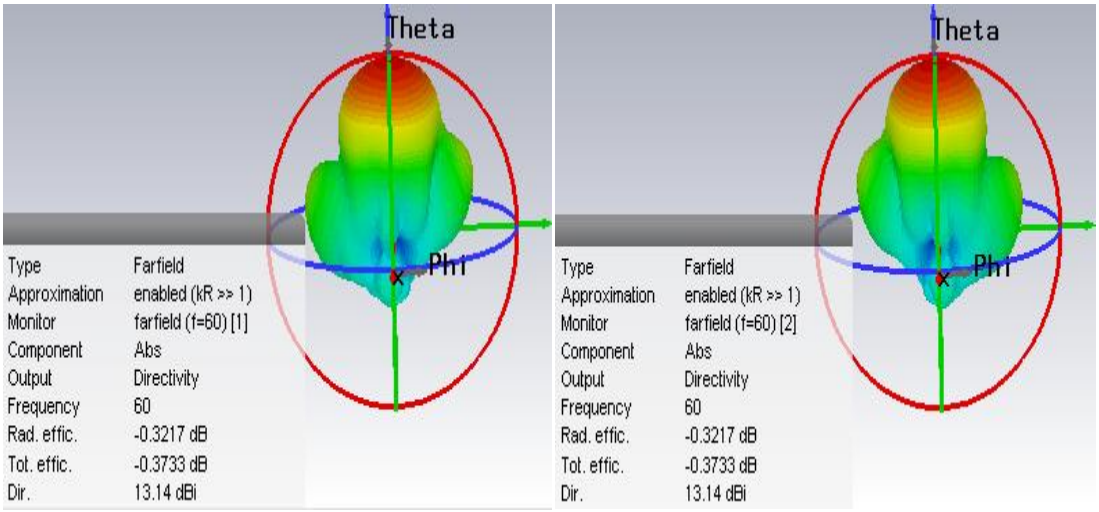


a) Antenna 1 b) Antenna 2

Fig. 3.21 3D directivity plot of an antenna a) and b) with spacing less than $\lambda_0/2$

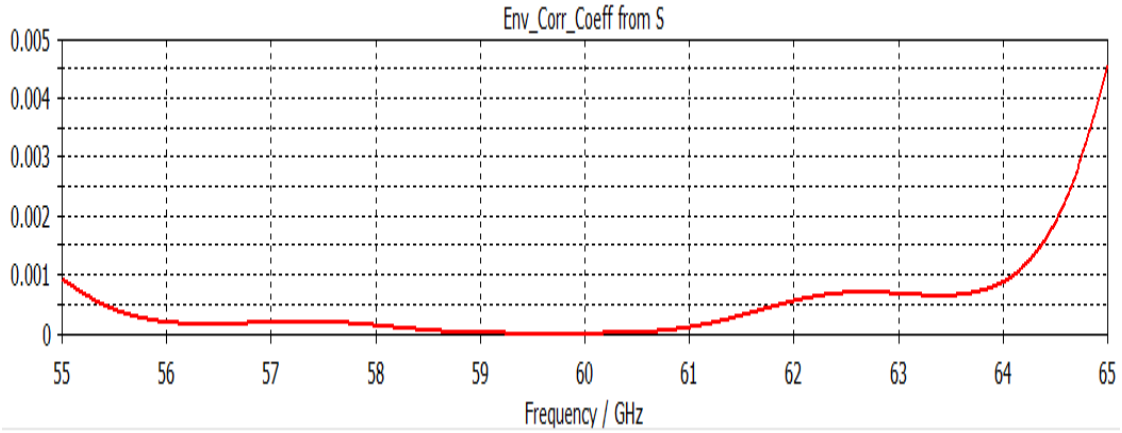


Fig. 3.22 Envelope Correlation Coefficient between antenna 1 and 2 with spacing less than $\lambda_0/2$

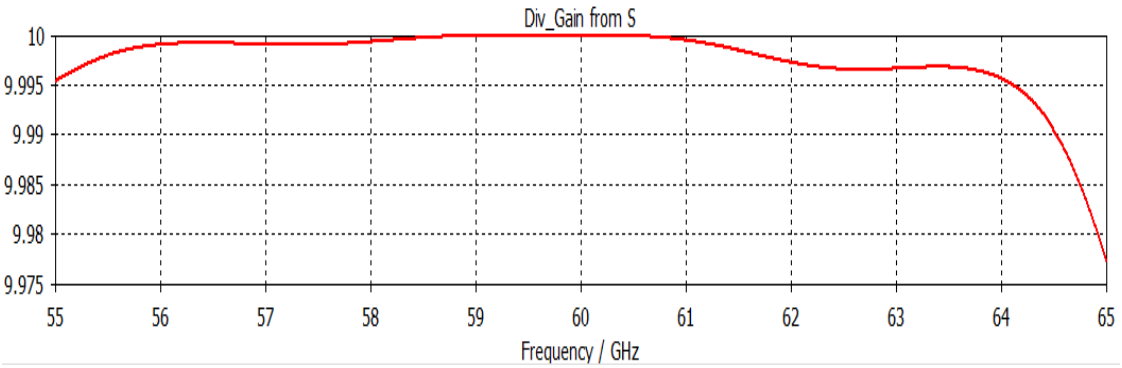


Fig. 3.23 Diversity gain of antenna 1 and 2 with spacing less than $\lambda_0/2$

From simulated results for the spacing less than $\lambda_0/2$ following conclusions are drawn, it can seen from simulation result that reducing the spacing between antenna array increases the mutual coupling which deteriorate the antenna performances.

Comparison between antenna elements with spacing greater than λ and less than λ/2 is tabulated in table 4.1

TABLE 3.4 Comparison of antenna characteristics with spacing greater than λ and less than λ/2

| **Parameters** | **Antenna spacing greater than λ** | **Antenna spacing less than λ/2** |
|---|---|---|
| **Return loss ($S_{11}$, $S_{22}$) (dB)** | -50.459 | -34.323 |
| **Transmission coefficient ($S_{12}$, $S_{21}$) (dB)** | < -35 | < -21.812 |
| **Resonant frequency (GHz)** | 60.48 | 60.43 |
| **Bandwidth (GHz)** | 4.701 | 4.5778 |
| **Frequency range (GHz)** | 58.322 – 63.023 | 58.434 – 63.012 |
| **Directivity (dBi)** | 13.73 | 13.2 |
| **ECC** | < 0.00001 | < 0.0005 |
| **Directive gain** | 9.9999 | 9.9995 |

From table 3.4 following conclusions can be drawn by reducing the spacing from $\lambda_0$ to $\lambda_0/2$

- Return loss increases by 16 dB which mean reflection increases
- Mutual coupling increases
- Resonant frequency shifts
- Matching Bandwidth decreases from 4.7 GHz to 4.5 GHz
- Frequency range compresses
- Directivity decreases
- Correlation increases
- Directive gain decreases

## 3.7 Isolation enhancement between antenna arrays using SMLR

Isolation techniques are developed to remove the mutual coupling. One of the technique is slotted meander line resonator. Isolation between antenna array using SMLR is shown in fig. 3.24 when the spacing between antennas is 1.524mm.

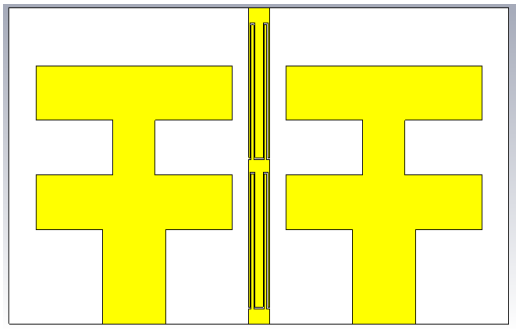

Fig. 3.24 Proposed design of antenna array having SMLR for isolation

The SMLR acts as a electrical resonator because of the oscillation of current induced within the slot. The SMLR is constructed by creating defect in a simple microstrip patch. The length and width of SMLR is 8.314 mm and 0.6mm, respectively. The gap between the SMLR is 0.09 mm. The gap between SMLR perturbs the surface current. The SMLR structure is shown in fig. 3.25.

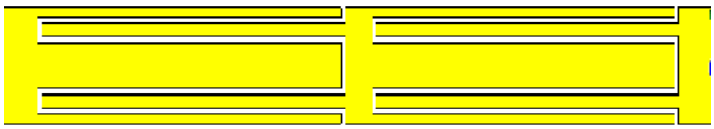

Fig. 3.25 SMLR decoupling unit

The simulation results are as follows

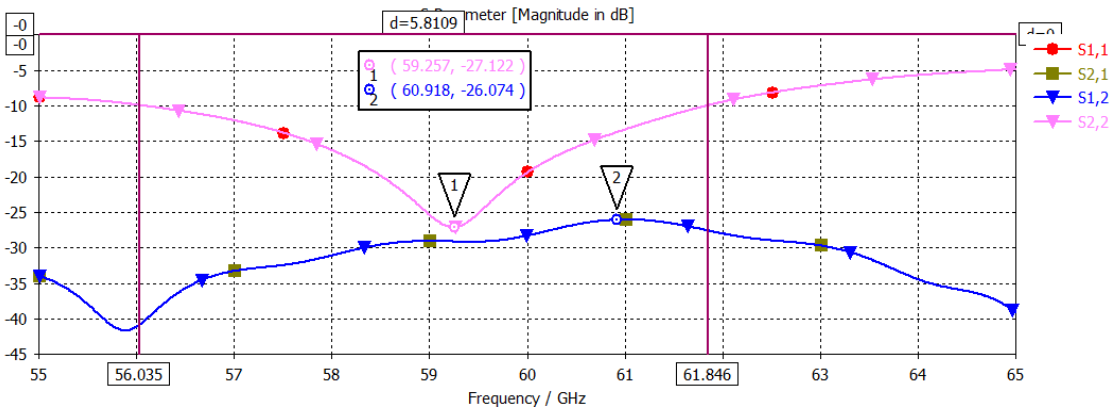


Fig. 3.26 Reflection and transmission coefficient of antenna having SMLR

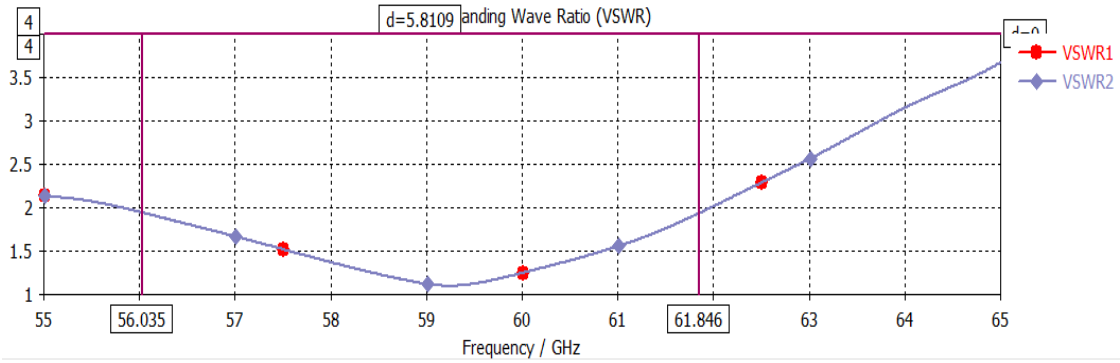


Fig. 3.27 VSWR of antenna having SMLR

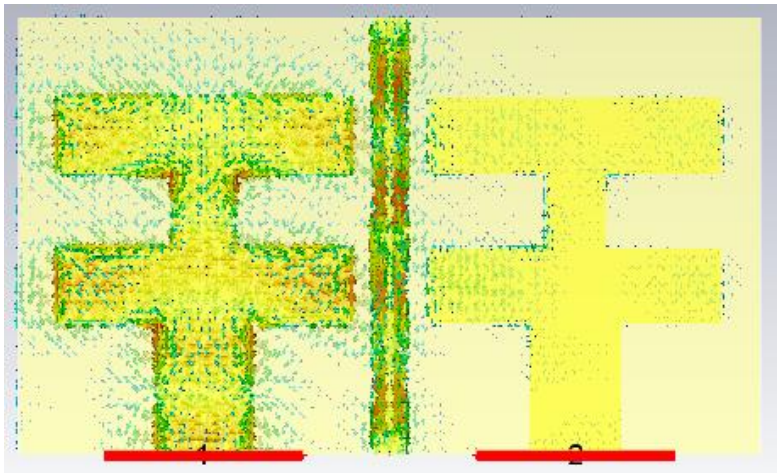

Fig. 3.28 Surface current at 60 GHz using SMLR

From fig. 3.28, the surface current from antenna 1 to antenna 2 is perturbed by the SMLR. The SMLR decouples the coupling wave.

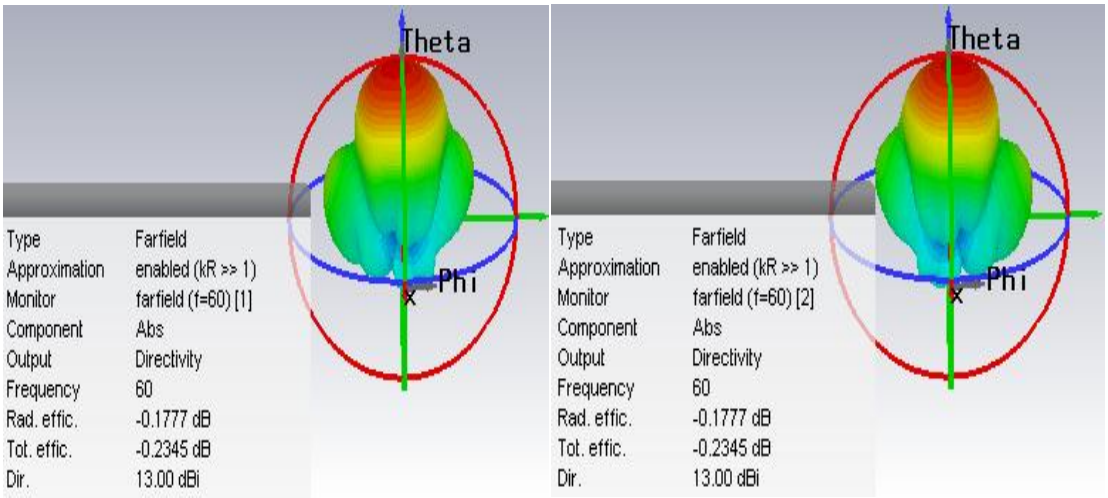


Fig. 3.29 3D directivity plot of an antenna 1 and 2 having SMLR for isolation

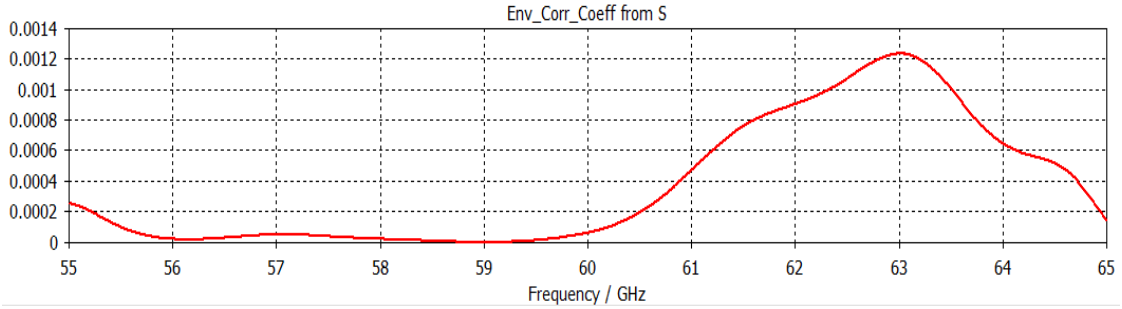


Fig. 3.30 ECC of an antenna with SMLR

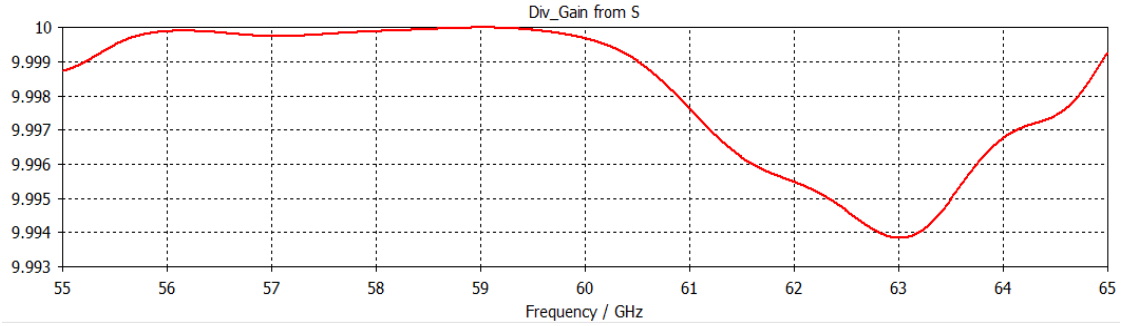


Fig. 3.31 DG of an antenna with SMLR

## 3.7 Isolation enhancement between antenna arrays using Metamaterial

Metamaterial provides isolation between microwave circuit elements such as multiple input multiple output (MIMO) systems. It has the property of negative electric permittivity and negative magnetic permeability. Mathematically, permittivity and permeability of a material can be calculated from S-parameters.

$$n = \frac{1}{Kd}\cos^{-1}\left[\frac{1}{2S_{11}}\left(1 - S_{11}^2 + S_{21}^2\right)\right]$$

$$Z = \sqrt{\frac{(1+S_{11})^2 - S_{21}^2}{(1-S_{11})^2 - S_{21}^2}}$$

Permittivity, $\varepsilon = \frac{n}{Z}$

Permeability, $\mu = nZ$

$K$ = wave vector of propagating wave

The MIMO antenna utilizes metamaterial for isolation improvement as shown in fig. 3.32 and the structure of metamaterial is depicted in fig. 3.33

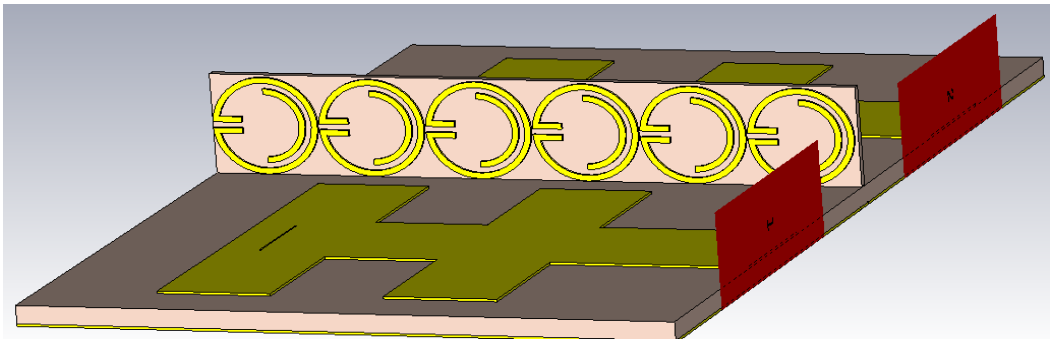

Fig. 3.32 Microstrip patch antenna using Metamaterial isolator

The metamaterial is constructed on substrate wall which is same as substrate material used above.

Height of substrate wall = 1.4 mm

Thickness of substrate wall = 1 mm

Total area of metamaterial between two array elements is $8.314 \times 1\ mm^2$.

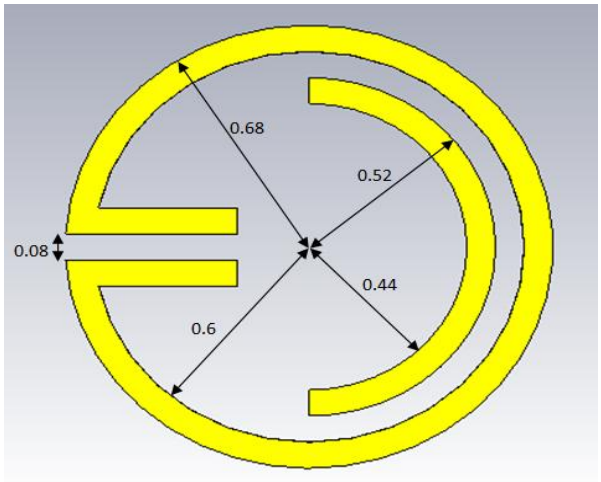


Fig. 3.33 Metamaterial structure

- The conductive part in metamaterial creates inductance.
- The gap in the ring creates capacitance effect.
- Semicircular ring enhances the bandwidth of the resonator over the desired band.

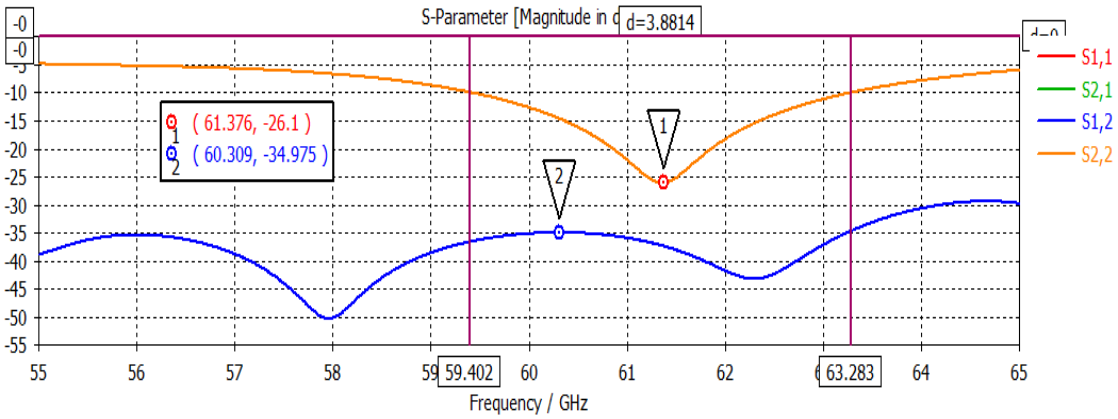


Fig. 3.34 Reflection and transmission coefficient of antenna having metamaterial

From fig.3.34, the reflection coefficient and transmission coefficient of MIMO antenna array at 60 GHz is -26.1 dB and -34.975 dB, respectively. the bandwidth of the desired MIMO antenna is 3.8814 GHz.

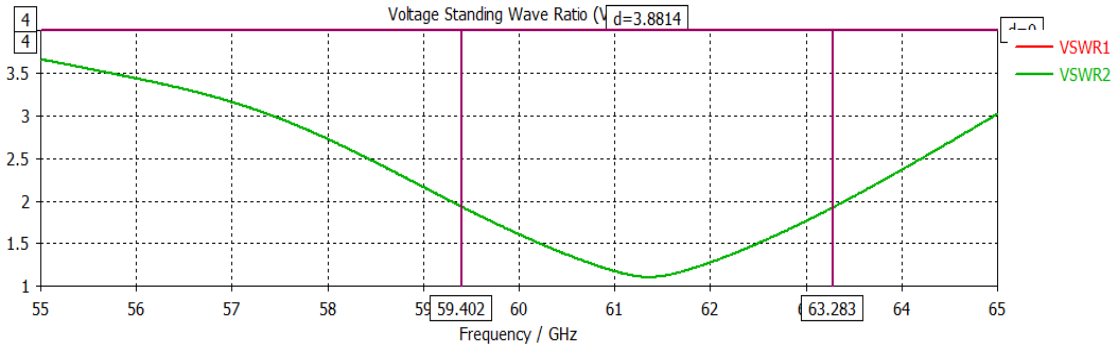


Fig. 3.35 VSWR of antenna having metamaterial

From fig. 3.35, the VSWR of desired antenna is less than 2. Ideally the VSWR should be 1 but practically it is diffcult to achieve. So, practically the VSWR should be less than 2.

The surface current distribution as depicted in fig. 3.36 demonstrates that the surface current excited at antenna 1 is not distrubing the antenna 2.

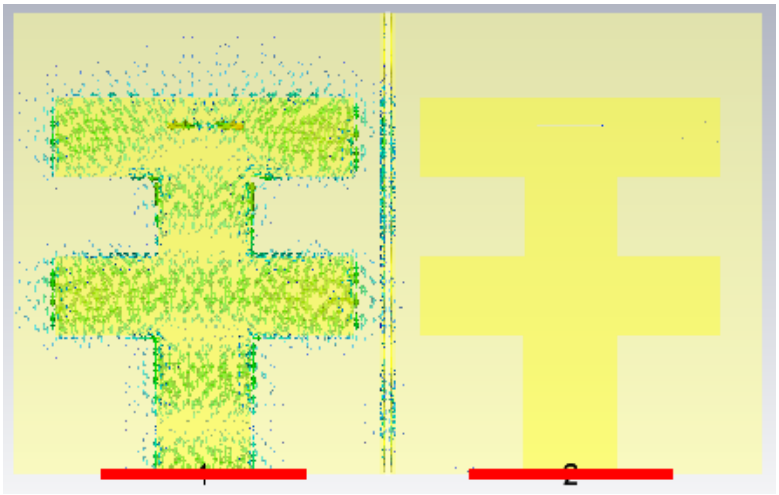


Fig. 3.36 Surface current of an antenna with metamaterial

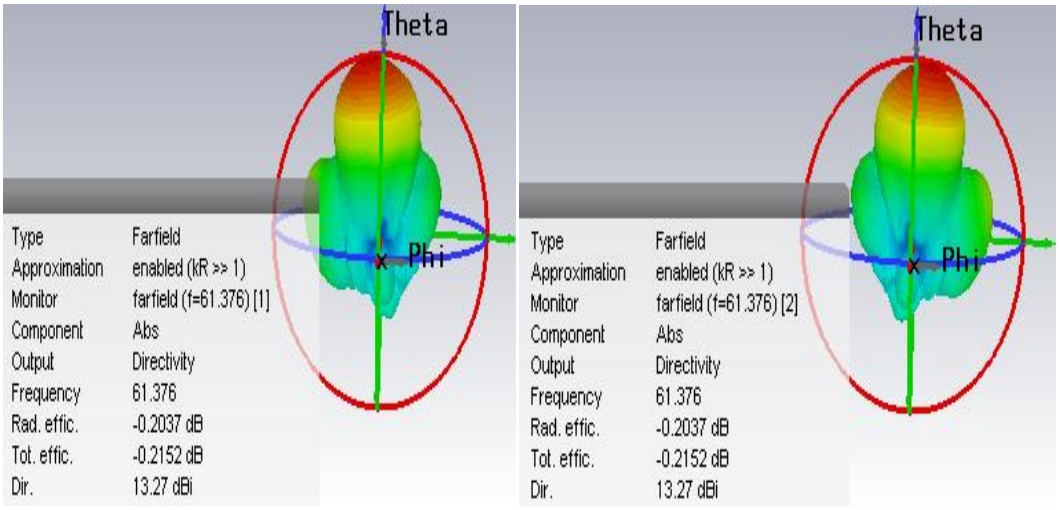


Fig. 3.37 3D directivity plot of antenna 1 and 2 having Metamaterial for isolation

The 3D directivity plot of antenna elements as shown in fig. 3.37 shows the directivity of an antenna 13.27 dBi.

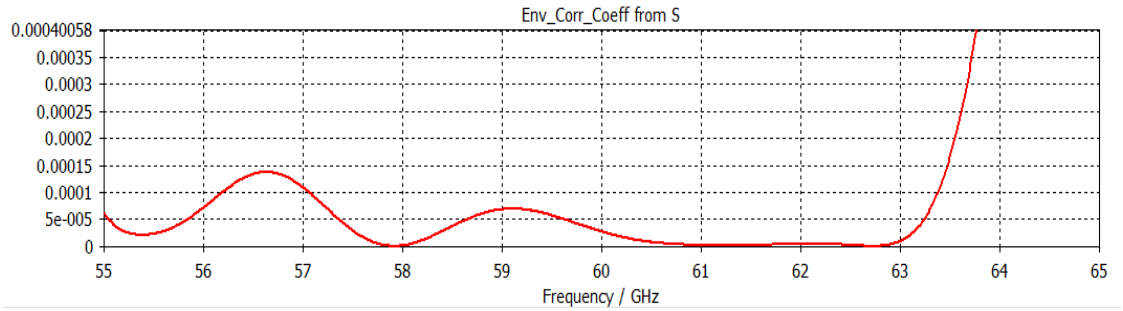


Fig. 3.38 ECC of antenna having metamaterial

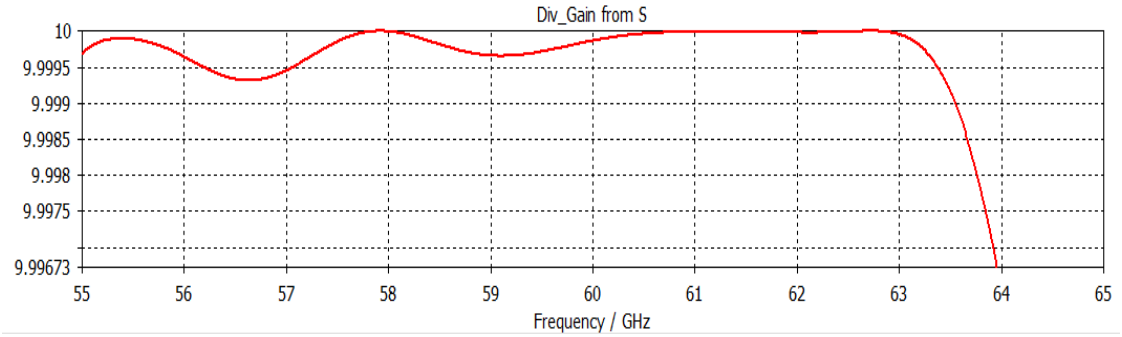


Fig. 3.39 DG of antenna having metamaterial

By comparing results of SMLR and Metamaterial for isolation enhancement are given in table 3.5

TABLE 3.5 Comparison of antenna characteristics with using SMLR and Metamaterial

| **Parameters** | **Using SMLR** | **Using Metamaterial** |
|---|---|---|
| **Return loss ( $S_{11}, S_{22}$ )(dB)** | -27.122 | -26.1 |
| **Transmission coefficient ( $S_{12}, S_{21}$ ) (dB)** | -26.074 | -34.975 |
| **VSWR** | < 2 | < 2 |
| **Resonant frequency (GHz)** | 59.257 | 61.376 |
| **Bandwidth (GHz)** | 5.8109 | 3.8814 |
| **Directivity (dBi)** | 13 | 13.27 |
| **ECC** | < 0.001 | < 0.00015 |
| **Directive gain** | > 9.995 | > 9.999 |

**Conclusion :**

Isolation using metamaterial is 11 dB more than SMLR. It increases the isolation on the cost of decreasing matching bandwidth. The bandwidth decreases by 2 GHz in metamaterial as compare to SMLR.

## 3.8 Proposed antenna design of 1 × 4 MIMO antenna

To increase the capacity of channel for high data rate, 1×4 antenna is constructed on the same substrate RT Duroid as used in section 3.1. For isolation between the antenna array SMLR is used. Proposed design 1×4 MIMO antenna using SMLR depicted in fig. 3.40 with spacing less than $\lambda_0/2$ i.e. 1.524 mm. The total area of 1 × 4 MIMO system is $28.37 \times 8.314\, mm^2$.

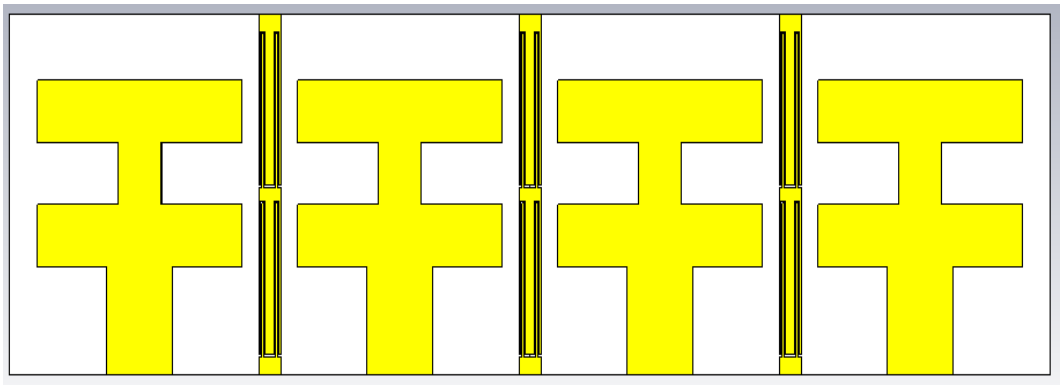

Fig . 3.40 Proposed design of 1 × 4 MIMO antenna using SMLR.

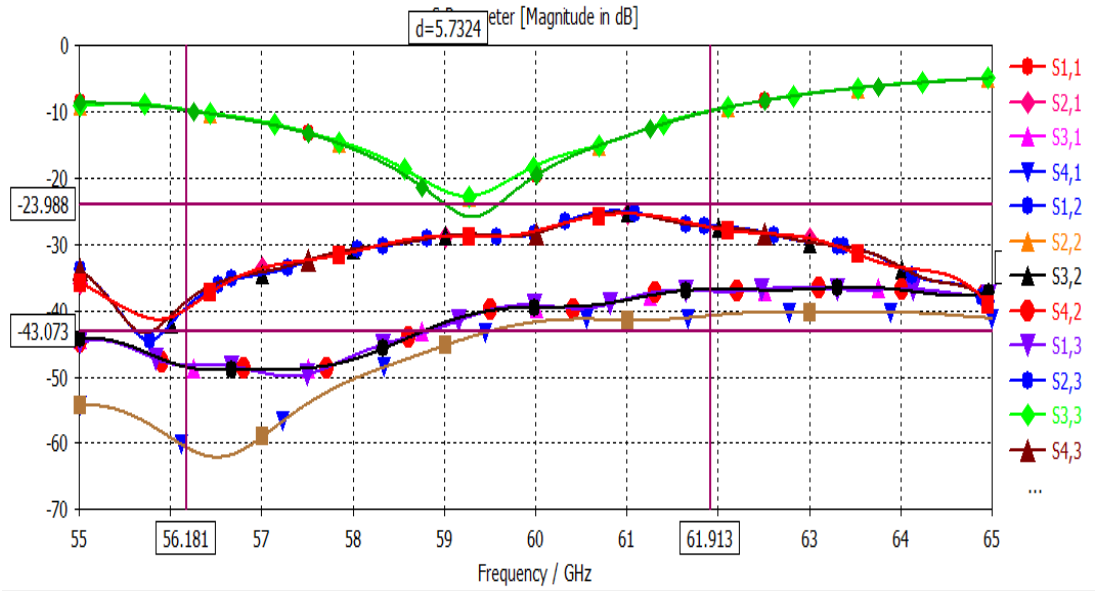


Fig. 3.41 Reflection and transmission coefficient of 1×4 antenna

Antenna characteristics such as return loss and transmission coefficient is shown in fig. 3.41. From fig.3.41, bandwidth = 5.5642 GHz, resonant frequency = 59.266 GHz, $f_H$ = 61.886 GHz, $f_L$ = 56.301GHz, return loss less than -23.9 dB, transmisssion coeffcient less than -25 dB. The isolation is less for the antenna 2 and 3 as compare to

antenna 1 and 4. The reason behind it, both the neighbour of antenna 2 and 3 are radiating i.e. 1 and 4. The energy is coupled at antenna 2 from antenna1 and 3. Similarly, the energy is coupled at antenna 3 from antenna 2 an4.

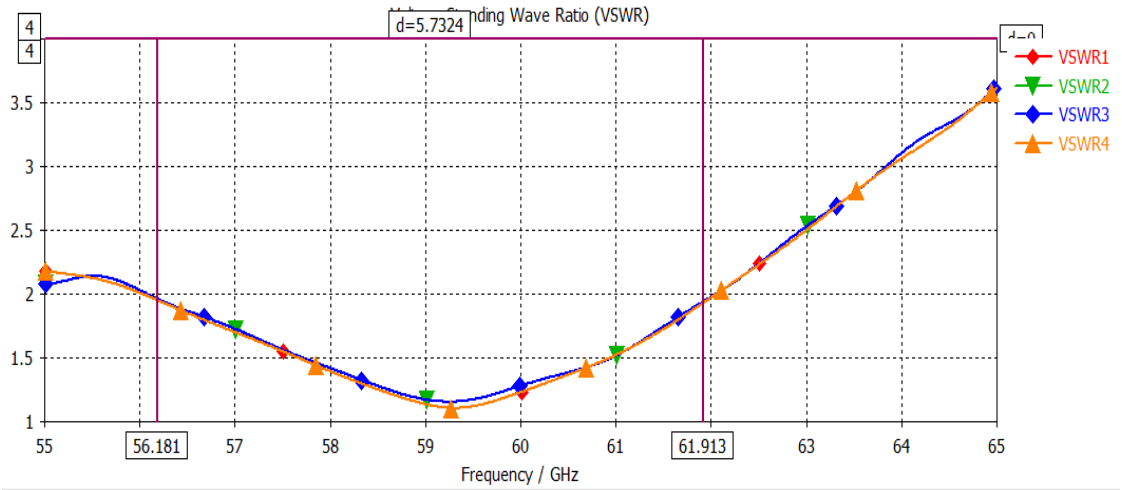


Fig. 3.42 VSWR of 1×4 antenna

The antenna 1×4 is having VSWR less than 2 as shown in fig. 3.42. To improve the isolation between the antenna array of 1×4, SMLR is constructed between antennas. The SMLR acts as decoupling unit between antennas. SMLR creates the obstacle in the path of oscillating current from one unit cell to another unit cell.

TABLE 3.6 Performance characteristics of Four element single band antennas without isolation

| **Parameters** | **Elements 1 and 2** | **Elements 2 and 3** | **Elements 1 and 3** | **Elements 1 and 4** |
|---|---|---|---|---|
| **(ECC)** | 0.00063 | 0.0006154 | 0.0000547 | 0.00004 |
| **(DG) (dB)** | 9.9969 | 9.9966 | 9.99973 | 9.9998 |

TABLE 3.7 Performance characteristics of four element single band antennas with isolation strip SMLR

| **Parameters** | **Elements 1 and 2** | **Elements 2 and 3** | **Elements 1 and 3** | **Elements 1 and 4** |
|---|---|---|---|---|
| **(ECC)** | < 0.0001 | < 0.001 | < 0.00008 | < 0.00005 |
| **(DG) (dB)** | 9.9979 | 9.997 | 9.9997 | 9.99995 |

The MIMO 1×4 antenna characteristics with and without isolation is tabulated in table 3.6 and 3.7. The correlation coefficient decreases and diversity gain increases by using isolation technique SMLR.

# CHAPTER-4

# CONCLUSION

## 4.1 Conclusion

The I-shaped patch antenna is designed at 60GHz for 5G wireless communication. Results are analyzed by varying slot length to $\lambda$, $\lambda/2$, $\lambda/4$, $\lambda/8$ and without slot length in the upper arm of I- shaped patch antenna. The dimensions (upper arm and lower arm width) of the antenna is optimized for the MIMO application, and the optimized results lead antenna to resonant at frequency 60.49, gain 13.2dBi, return loss -50.319dB and matching bandwidth 4.6674GHz for upper arm length 1.7 mm and lower arm length 1.75mm. By using these optimized dimensions, the antenna array (1×2) is created. To remove mutual coupling between antenna array, isolation techniques SMLR and metamaterial are used. The comparative study is done between these two isolation techniques. Metamaterial has isolation 10 dB more than SMLR. Metamaterial increases the isolation on the cost of decreasing matching bandwidth.

After designing of a 1×2 array, to increase the capacity of channel 1×4 array is designed using SMLR. The area covered by geometry of 1×4 is $28.37 \times 8.314\, mm^2$ .The ECC of the antenna elements between 1 and 2, 1 and 3, 2 and 3, and 1 and 4 is very low. The diversity gain is high (>9.997).

## 5.2 Future work

Since we know that after putting all best efforts there is always a scope to improve the characteristics of the antenna. Thus, in our design, the future scope is also available to make it ideal for 60 GHz MIMO application. This can be achieved by improving isolation techniques.

# REFERENCES


[1] C. H. See, R. A. Abd-Alhameed, Z. Z. Abidin, N. J. McEwan, & P. S. Excell, "Wideband printed MIMO/diversity monopole antenna for WiFi/WiMAx applications," *IEEE transactions on antennas and propagation*, vol. 60, no.4, pp. 2028-2035, 2012.

[2] S. Hwangbo, H. Y. Yang, & Y. K. Yoon,"Mutual Coupling Reduction using Micromachined Complementary Meander Line Slots for a Patch Array Antenna," *IEEE Antennas and Wireless Propagation Letters*, vol. 16, pp. 1667-1670, 2017.

[3] M. R. Devi, C. Poongodi, & D. Deepa, "Comparison slotted meander line resonators and P-EBG structures in microstrip patch antennas with isolation enhancement for wimax applications," *2014 International Conference on Green Computing Communication and Electrical Engineering (ICGCCEE),* pp. 1-5, 2014.

[4] A. Dadgarpour, B. Zarghooni, & T. A. Denidni, "Mutual-coupling suppression for 60 GHz MIMO antenna using metamaterials," *2015 IEEE International Symposium on Antennas and Propagation & USNC/URSI National Radio Science Meeting,*. pp. 422-423, 2015.

[5] X. M. Yang, X. G. Liu, X. Y. Zhou, & T. J. Cui, "Reduction of mutual coupling between closely packed patch antennas using waveguided metamaterials," *IEEE Antennas and Wireless Propagation Letters*, vol. 11, pp. 389-391, 2012.

[6] M. L.Morales, J. Hirokawa, & M. Sierra-Castañer, "Control of phase in radial line slot antenna for 5G communications at 60GHz,"*11th European Conference on* In *Antennas and Propagation (EUCAP),* pp. 3738-3742, Mar. 2017.

[7] X. Li, B. B. Xu, & H. L. Peng, "A 60GHz antenna array with heatsink considerations for massive-MIMO applications," *Electrical Design of Advanced Packaging and Systems (EDAPS),* pp. 79-81, Dec. 2016

[8] H. Sato, T. Hayashi, Y. Koyanagi, & H. Morishita, "Small array antenna for 2x2 MIMO terminal using folded loop antenna," *Antennas and Propagation, 2006. EuCAP 2006. First European Conference on*, pp. 1-5, Nov. 2006.

[9] Y. Al-Ajrawi, & J. Rahhal, "A simple antenna design for massive MIMO techniques," *Electrical and Electronics Engineering Conference (JIEEEC), 2015 9th Jordanian International*, pp. 1-7, Oct. 2015.

[10] A. A. Isaac, H. M. Al-Rizzo, A. I. Hammoodi, S. Abushamleh, & H. R. Khaleel, "Isolation enhancment of two planar monopole antennas for MIMO wireless applications," *Antennas and Propagation & USNC/URSI National Radio Science Meeting*, pp. 380-381, Jul. 2015.

[11] S. H. Jeong, H. H. Cho, & O. H. Jeong, "Study of Multiple Antenna Placement Used in Mobile Device," In *ITC-CSCC: International Technical Conference on Circuits Systems, Computers and Communications*, pp. 701-702, Jun. 2015.

[12] C. A. Balanis, *Antenna Theory, Analysis and Design*, Second Edition: John Wiley and Sons, Inc., New York, 1997.

[13] A. Jain, P. K. Verma, & V. K. Singh, " Performance analysis of PIFA based 4× 4 MIMO antenna," *Electronics letters*, vol. *48*, no. 9, pp. 474-475, 2012.

[14] https://www.cst.com/

[15] K. K. Sharma, & R. K. Goyal, "Slotted microstrip patch antenna at 60GHz for point to point communication," In *Communication Networks (ICCN), 2015 International Conference on* , pp. 371-373, Nov. 2015.

[16] R. Karimian, A. Kesavan, M. Nedil, & T. A. Denidni, "Low-Mutual-Coupling 60-GHz MIMO Antenna System With Frequency Selective Surface Wall," *IEEE Antennas and Wireless Propagation Letters*, vol. 16, pp. 373-376, 2017.

[17] G. Han, L. Han, R. Ma, Q. Zeng, & W. Zhang, "A novel MIMO antenna with DGS for high isolation," In *Numerical Electromagnetic and Multiphysics Modeling and Optimization (NEMO), 2016 IEEE MTT-S International Conference on* , pp. 1-2, Jul. 2016.

[18] H. Qi, L. Liu, X. Yin, H. Zhao, & W. J. Kulesza, "Mutual coupling suppression between two closely spaced microstrip antennas with an asymmetrical coplanar strip wal,l" *IEEE Antennas and Wireless Propagation Letters*, vol. 15, pp. 191-194, 2016.

[19] A. C. J. Malathi, & D. Thiripurasundari, "Review on isolation techniques in MIMO antenna systems," *Indian Journal of Science and Technology*, vol. 9, *pp.* 35, 2016.

[20] M. Niroo-Jazi, T. A.Denidni, M. R. Chaharmir, & A. R. Sebak, "A hybrid isolator to reduce electromagnetic interactions between Tx/Rx antennas," *IEEE Antennas and Wireless Propagation Letters*, vol. 13, pp. 75-78, 2014.

[21] M. G. N. Alsath, , M. Kanagasabai, & B. Balasubramanian, "Implementation of slotted meander-line resonators for isolation enhancement in microstrip patch antenna arrays," *IEEE Antennas and Wireless Propagation Letters*, vol. 12, pp. 15-18, 2013.

[22] R. Hoque, M. Asaduzzaman, I. Hossain, F. Imteaz, & U. Saha, "Distinguishing performance of 60-GHz microstrip patch antenna for different dielectric materials," In *Electrical Engineering and Information & Communication Technology (ICEEICT), 2014 International Conference on* , pp. 1-4, Apr. 2014.

[23] A. S. Chauhan & R. Ramesh, "Efficient method of increase in isolation between patch antennas using metamaterial," In *Communications and Signal Processing (ICCSP), 2015 International Conference on* , pp. 0205-0208, Apr. 2015.

[24] H. Qi, X. Yin, L. Liu, Y. Rong, & H. Qian, "Improving isolation between closely spaced patch antennas using interdigital lines," *IEEE Antennas and Wireless Propagation Letters*, vol. 15, pp. 286-289, 2016

[25] H. S. Farahani, M. Veysi, M. Kamyab, & A. Tadjalli, "Mutual coupling reduction in patch antenna arrays using a UC-EBG superstrate," *IEEE Antennas and Wireless Propagation Letters*, vol. 9, pp. 57-59, 2010.

[26] R.Hafezifard, M. Naser-Moghadasi, J.R. Mohassel, J. R., & R. A.Sadeghzadeh, "Mutual coupling reduction for two closely spaced meander line antennas using metamaterial substrate," *IEEE Antennas and Wireless Propagation Letters*, vol. 15, pp. 40-43, 2016.

[27] S. Kamal, & A. A. Chaudhari, "Printed Meander Line MIMO Antenna Integrated with Air Gap, DGS and RIS: A Low Mutual Coupling Design for LTE Applications," *Progress In Electromagnetics Research C*, vol. 71, pp. 149-159, 2017.

[28] Y. Lee, D. Ga, & J. Choi, "Design of a MIMO antenna with improved isolation using MNG metamaterial," *International Journal of Antennas and Propagation*, 2012.

[29] C. M. Luo, J. S. Hong, & L. L. Zhong, "Isolation enhancement of a very compact UWB-MIMO slot antenna with two defected ground structures," *IEEE Antennas and Wireless Propagation Letters*, vol. 14, pp. 1766-1769, 2015

[30] J. Y. Deng, L. X. Guo, & X. L. Liu, "An ultrawideband MIMO antenna with a high isolation," *IEEE Antennas And Wireless Propagation Letters*, vol. 15, pp. 182-185, 2016.

[31] Y. E. Al-Shaikh, & L. A. Salman, "Design of a Metamaterial Enhanced Triple Band Printed MIMO Antenna for WiFi and WiMAx Applications," *International Journal of Science, Engineering and Computer Technology*, vol. *6*, pp. 11, no. 380, 2016

[32] R. K. Goyal & K. K. Sharma, "T-slotted microstrip patch antenna for 5G Wi-Fi network," In *Advances in Computing, Communications and Informatics (ICACCI), 2016 International Conference on* , pp. 2684-2687, Sept. 2016

[33] Y. L. Ban, Z. X. Chen, Z. Chen, K. Kang, & J. L. W. Li, "Decoupled hepta-band antenna array for WWAN/LTE smartphone applications," *IEEE Antennas and Wireless Propagation Letters*, vol. 13, pp. 999-1002, 2014

[34] X. Ruan, S. W. Qu, Q. Zhu, K. B. Ng, & C. H. Chan, "A Complementary Circularly Polarized Antenna for 60-GHz Applications," *IEEE Antennas and Wireless Propagation Letters*, vol. 16, pp. 1373-1376, 2017.

# PUBLICATION

---

Durga Kumari, K. K. Sharma, "Improved Isolation Between Antennas using Slotted Meander Line Structure for 5G Wireless Applications*," IEEE International Conference on Computer, Communications and Electronics, Jaipur, July 01-02, 2017.*

# Thesis

ORIGINALITY REPORT

| %19 | %11 | %11 | %12 |
|---|---|---|---|
| SIMILARITY INDEX | INTERNET SOURCES | PUBLICATIONS | STUDENT PAPERS |

PRIMARY SOURCES

| | | |
|---|---|---|
| 1 | Submitted to Punjab Technical University<br>Student Paper | %1 |
| 2 | www.ukessays.com<br>Internet Source | %1 |
| 3 | Submitted to University of Northumbria at Newcastle<br>Student Paper | %1 |
| 4 | Ravi Kumar Goyal, K. K. Sharma. "T-slotted microstrip patch antenna for 5G Wi-Fi network", 2016 International Conference on Advances in Computing, Communications and Informatics (ICACCI), 2016<br>Publication | %1 |
| 5 | Yong-Ling Ban, , Zhong-Xiang Chen, Zhi Chen, Kai Kang, and Joshua Le-Wei Li. "Decoupled Hepta-Band Antenna Array for WWAN/LTE Smartphone Applications", IEEE Antennas and Wireless Propagation Letters, 2014.<br>Publication | %1 |
| | Xuexuan Ruan, Shi-Wei Qu, Qian Zhu, Kung | |

| | | |
|---|---|---|
| 6 | Bo Ng, Chi Chan. "A Complementary Circularly Polarized Antenna for 60-GHz Applications", IEEE Antennas and Wireless Propagation Letters, 2016<br>Publication | %1 |
| 7 | ethesis.nitrkl.ac.in<br>Internet Source | <%1 |
| 8 | ijccts.org<br>Internet Source | <%1 |
| 9 | Submitted to Jawaharlal Nehru Technological University Kakinada<br>Student Paper | <%1 |
| 10 | Submitted to Amity University<br>Student Paper | <%1 |
| 11 | Submitted to Savitribai Phule Pune University<br>Student Paper | <%1 |
| 12 | Jain, A., P.K. Verma, and V.K. Singh. "Performance analysis of PIFA based 4×4 MIMO antenna", Electronics Letters, 2012.<br>Publication | <%1 |
| 13 | Submitted to The University of Manchester<br>Student Paper | <%1 |
| 14 | Submitted to Higher Education Commission Pakistan<br>Student Paper | <%1 |

| | | |
|---|---|---|
| 15 | Majid Manteghi. "A novel miniaturized triband PIFA for MIMO applications", Microwave and Optical Technology Letters, 03/2007<br>Publication | <%1 |
| 16 | bradscholars.brad.ac.uk<br>Internet Source | <%1 |
| 17 | Submitted to University of Nottingham<br>Student Paper | <%1 |
| 18 | etd.lib.fsu.edu<br>Internet Source | <%1 |
| 19 | Dadgarpour, Abdolmehdi, Behnam Zarghooni, and Tayeb A. Denidni. "Mutual-coupling suppression for 60 GHz MIMO antenna using metamaterials", 2015 IEEE International Symposium on Antennas and Propagation & USNC/URSI National Radio Science Meeting, 2015.<br>Publication | <%1 |
| 20 | Submitted to Universiti Malaysia Sarawak<br>Student Paper | <%1 |
| 21 | Submitted to Madan Mohan Malaviya University of Technology<br>Student Paper | <%1 |
| 22 | Luo, Chao-Ming, Jing-Song Hong, and Lin-Lin Zhong. "Isolation Enhancement of a Very | <%1 |

| | | |
|---|---|---|
| | Compact UWB-MIMO Slot Antenna With Two Defected Ground Structures", IEEE Antennas and Wireless Propagation Letters, 2015.<br>Publication | |
| 23 | ijarece.org<br>Internet Source | <%1 |
| 24 | www.ijsr.net<br>Internet Source | <%1 |
| 25 | Submitted to University of Bedfordshire<br>Student Paper | <%1 |
| 26 | www.andrew.cmu.edu<br>Internet Source | <%1 |
| 27 | Submitted to Panjab University<br>Student Paper | <%1 |
| 28 | Alsath, G., M. Kanagasabai, and B. Ramani. "Implementation of Slotted Meander Line Resonators for Isolation Enhancement in Microstrip Patch Antenna Arrays", IEEE Antennas and Wireless Propagation Letters, 2012.<br>Publication | <%1 |
| 29 | Submitted to Indian Institute of Technology Jodhpur<br>Student Paper | <%1 |
| 30 | Submitted to University Tun Hussein Onn | <%1 |

| | | |
|---|---|---|
| | Malaysia<br>Student Paper | |
| 31 | etheses.whiterose.ac.uk<br>Internet Source | <%1 |
| 32 | Submitted to Eastern Mediterranean University<br>Student Paper | <%1 |
| 33 | Shankar Singh, Hari, Gaurav Kumar Pandey, Pradutt Kumar Bharti, and Manoj Kumar Meshram. "Design and performance investigation of a low profile MIMO/Diversity antenna for WLAN/WiMAX/HIPERLAN applications with high isolation : Investigation of Low Profile MIMO Antenna", International Journal of RF and Microwave Computer-Aided Engineering, 2015.<br>Publication | <%1 |
| 34 | eprints.utm.my<br>Internet Source | <%1 |
| 35 | dspace.nitrkl.ac.in<br>Internet Source | <%1 |
| 36 | lib.znate.ru<br>Internet Source | <%1 |
| 37 | Submitted to National Institute of Technology Karnataka Surathkal<br>Student Paper | <%1 |

| | | |
|---|---|---|
| 38 | Kuttathati Srinivasan Vishvaksenan, Kaliyappa Mithra, Ramalingam Kalaiarasan, Kaliyappa Santhosh Raj. "Mutual Coupling Reduction in Microstrip Patch Antenna Arrays Using Parallel Coupled-Line Resonators", IEEE Antennas and Wireless Propagation Letters, 2017<br>Publication | <%1 |
| 39 | Velan, Sangeetha, Chinnambeti Raviteja, M. Gulam Nabi Alsath, Aswathy K. Sarma, Henridass Arun, and Malathi Kanagasabai. "Polarisation diverse multiple input–multiple output antenna with enhanced isolation", IET Microwaves Antennas & Propagation, 2015.<br>Publication | <%1 |
| 40 | Submitted to Universiti Teknikal Malaysia Melaka<br>Student Paper | <%1 |
| 41 | Submitted to Wilkes University<br>Student Paper | <%1 |
| 42 | dyuthi.cusat.ac.in<br>Internet Source | <%1 |
| 43 | Submitted to Sreenidhi International School<br>Student Paper | <%1 |
| 44 | Submitted to Tufts University<br>Student Paper | <%1 |

| | | |
|---|---|---|
| 45 | cst.com<br>Internet Source | <%1 |
| 46 | www.deepdyve.com<br>Internet Source | <%1 |
| 47 | Naser-Moghadasi, M., R. Hafezifard, R. A. Sadeghzadeh, H. Seyyedhatami, and M. Torkamani. "Small circular-shaped UWB antenna for wireless communication applications", Microwave and Optical Technology Letters, 2012.<br>Publication | <%1 |
| 48 | Submitted to Indian Institute of Information Technology, Allahabad<br>Student Paper | <%1 |
| 49 | www.istp.org.in<br>Internet Source | <%1 |
| 50 | Submitted to City University<br>Student Paper | <%1 |
| 51 | Othman, Nur Nasyilla, Wan Noor Najwa Wan Marzudi, Nur Faizah Mohamad Yusof, Zuhairiah Zainal Abidin, Siti Zarina Mohamad Muji, and Yue Ma. "MIMO Antenna Performances on Microstrip Antenna with EBG Structure for WLAN Applications", Applied Mechanics and Materials, 2015.<br>Publication | <%1 |

| | | |
|---|---|---|
| 52 | Submitted to Institute of Graduate Studies, UiTM<br>Student Paper | <%1 |
| 53 | Submitted to Universiti Putra Malaysia<br>Student Paper | <%1 |
| 54 | Ultra-Wideband and 60 GHz Communications for Biomedical Applications, 2014.<br>Publication | <%1 |
| 55 | Turnitin 한국 DB, 국민대학교<br>Publication | <%1 |
| 56 | diva-portal.org<br>Internet Source | <%1 |
| 57 | Submitted to Indian School of Mines<br>Student Paper | <%1 |
| 58 | Submitted to Technological Educational Institution of Athens - Department of Electronics<br>Student Paper | <%1 |
| 59 | Submitted to University of Newcastle upon Tyne<br>Student Paper | <%1 |
| 60 | ICHINOSE, Takashi, and Masato WAKAYAMA. "SPECIAL VALUES OF THE SPECTRAL ZETA FUNCTION OF THE NON-COMMUTATIVE HARMONIC OSCILLATOR AND CONFLUENT | <%1 |

HEUN EQUATIONS", Kyushu Journal of Mathematics, 2005.
Publication

| | | |
|---|---|---|
| 61 | Submitted to University of Birmingham<br>Student Paper | <%1 |
| 62 | Transactions on Engineering Technologies, 2016.<br>Publication | <%1 |
| 63 | Allam, A.M.M.A, and Adham Mohamed Gamal Hemdan. "Novel DGS shape for mutual coupling reduction", 2016 German Microwave Conference (GeMiC), 2016.<br>Publication | <%1 |
| 64 | Ibrahim, Ahmed A., Mahmoud A. Abdalla, Adel B. Abdel-Rahman, and Hesham F. A. Hamed. "Compact MIMO antenna with optimized mutual coupling reduction using DGS", International Journal of Microwave and Wireless Technologies, 2013.<br>Publication | <%1 |
| 65 | repository.liv.ac.uk<br>Internet Source | <%1 |
| 66 | Submitted to Universiti Sains Malaysia<br>Student Paper | <%1 |
| 67 | Waelbroeck, Claire, Jean-Claude Duplessy, Elisabeth Michel, Laurent Labeyrie, Didier | <%1 |

Paillard, and Josette Duprat. "erratum: The timing of the last deglaciation in North Atlantic climate records", Nature, 2001.
Publication

| | | |
|---|---|---|
| 68 | Anitha Ramachandran, Sumitha Mathew, Vivek Rajan, Vasudevan Kesavath. "A Compact Tri-Band Quad Element MIMO Antenna Using SRR Ring for High Isolation", IEEE Antennas and Wireless Propagation Letters, 2016<br>Publication | <%1 |
| 69 | www.jpier.org<br>Internet Source | <%1 |
| 70 | ijafrc.org<br>Internet Source | <%1 |
| 71 | Communications in Computer and Information Science, 2013.<br>Publication | <%1 |
| 72 | Lingsheng Yang, Ming Ji, Biyu Cheng, Bo Ni. "Eight-Element Antenna Array for LTE 3.4–3.8 GHz Mobile Handset Applications", Frequenz, 2017<br>Publication | <%1 |
| 73 | www.i-scholar.in<br>Internet Source | <%1 |
| 74 | www.e-fermat.org<br>Internet Source | <%1 |

| | | |
|---|---|---|
| 75 | Submitted to KDU College Sdn Bhd<br>Student Paper | <%1 |
| 76 | Praveen Kumar, P. C., and P. Trinatha Rao. "Dual staircase shaped microstrip patch antenna", 2015 International Conference on Pervasive Computing (ICPC), 2015.<br>Publication | <%1 |
| 77 | Zhou, Rongguo, Duixian Liu, and Hao Xin. "A Wideband Circularly Polarized Patch Antenna for 60 GHz Wireless Communications", Wireless Engineering and Technology, 2012.<br>Publication | <%1 |
| 78 | docplayer.net<br>Internet Source | <%1 |
| 79 | Liu, Yan-Yan, and Zhi-Hong Tu. "Compact Differential Band-Notched Stepped-Slot UWB-MIMO Antenna with Common-Mode Suppression", IEEE Antennas and Wireless Propagation Letters, 2016.<br>Publication | <%1 |
| 80 | Proceedings of the International Conference on Recent Cognizance in Wireless Communication & Image Processing, 2016.<br>Publication | <%1 |
| 81 | Sharawi, Mohammad S.. "Printed Multi-Band MIMO Antenna Systems and Their | <%1 |

Performance Metrics [Wireless Corner]", IEEE Antennas and Propagation Magazine, 2013.
Publication

---

82 Yong-Ling Ban, Chuan Li, Chow-Yen-Desmond Sim, Gang Wu, Kin-Lu Wong. "4G/5G Multiple Antennas for Future Multi-Mode Smartphone Applications", IEEE Access, 2016 <%1
Publication

---

83 Abidin, Z. Z.(Abd-Alhameed, Raed A. and McEwan, Neil J.). "Design, modelling and implementation of antennas using electromagnetic bandgap material and defected ground planes. Surface Meshing Analysis and Genetic Algorithm Optimisation on EBG and Defected Ground Structures for Reducing the Mutual Coupling between Radiating Elements of Antenna Array and MIMO Systems.", University of Bradford, 2012. <%1
Publication

---

EXCLUDE QUOTES ON
EXCLUDE BIBLIOGRAPHY ON
EXCLUDE MATCHES OFF